A PHOTOMETRIC SEARCH AND ANALYSIS OF SHORT-PERIOD VARIABLE STARS IN THE OPEN CLUSTER NGC 7092

by

Sarah L. Schuff

A senior thesis submitted to the faculty of

Brigham Young University

in partial fulfillment of the requirements for the degree of

Bachelor of Science

Department of Physics and Astronomy

Brigham Young University

December 2007

BRIGHAM YOUNG UNIVERSITY

DEPARTMENT APPROVAL

of a senior thesis submitted by

Sarah L. Schuff

This thesis has been reviewed by the research advisor, research coordinator, and department chair and has been found to be satisfactory.

Date	Eric G. Hintz, Advisor
Date	Eric G. Hintz, Research Coordinator
Date	Ross Spencer, Chair

ABSTRACT

A PHOTOMETRIC SEARCH AND ANALYSIS OF SHORT-PERIOD VARIABLE STARS IN THE OPEN CLUSTER NGC 7092

Sarah L. Schuff

Department of Physics and Astronomy

Bachelor of Science

The open cluster NGC 7092 was observed over the course of 6 nights during the years 2004-2006. Five nights were taken from the 0.4 m David Derrick Telescope of the Orson Pratt Observatory at Brigham Young University in Provo, Utah. One other employed the 0.3 m telescope at West Mountain Observatory on West Mountain, Utah. All frames were taken using B, V, or R filters; data were analyzed in V using standard aperture photometry techniques. Series of short and long exposures were taken for comparison of surface as well as deep-field study. A total of 238 stars were studied and differential photometry techniques applied to determine variability. Of these, 15 are suspected short-period variables and 3 are known.

ACKNOWLEDGMENTS

To the people who keep me going—

This thesis would have never come about without the tireless help and support of a few key friends, mentors, and fellow astronomers. Many thanks go to Laura Adams, Danny Marini, Dave Broadbent [1], Tabitha Bush [2], and Kathleen Moncrieff [3]. To Laura, for her help in taking all that data up on West Mount, serving as an excellent hiking partner, and rescuing me from the rattlesnake; to Danny, for a year of encouragement and support; to Dave, for the life-saving donations of his LaTeX template and cheat-sheets; to Tabitha, for the late-night phone help and pizza; and to Kathleen, who literally devoted hours of her own free time to baby me through the workings of IRAF. One could not ask for better friends.

I would also like to thank Professor Mike Joner for the incredible opportunity he gave me in working up at West Mount Observatory over the spring, summer, and fall of 2006. Some of the most memorable moments of my life were made up there between the telescopes and the open night sky. Also thanks to him and his wife, Lisa Joner, for grabbing a few extra nights of M39 in between their other research. Thanks is also due to my advisor, Dr. Eric Hintz, for teaching me nearly everything I know about observational astronomy and for tirelessly attending to my barrage of questions.

I would like to express my most heartfelt gratitude to the House of Schuff - to my siblings, for keeping me happy and sane; to Mom, for reasons that would go on for pages; to all my grandparents, for their financial support through college and the

vicarious pleasure they received in everything I learned; and for Grandpa and his continual rallying cry to “Hang in there!”

Finally, I would like to dedicate this thesis to the memory of my dad, William Ray Schuff. His passion for the beauty and workings of the world around him inspired my own life’s direction. I still think he’s the smartest man in the world.

Contents

1 Introduction **1**
- 1.1 Why Astronomy . . . 1
- 1.2 Why Variable Stars . . . 2
- 1.3 Thesis Overview . . . 3

2 Background **5**
- 2.1 HJD . . . 5
- 2.2 Light Curves . . . 6
- 2.3 The Magnitude Scale . . . 6
- 2.4 Color . . . 7
- 2.5 Airmass/Extinction . . . 8
- 2.6 Photometric Nights—All-Sky Photometry . . . 8
- 2.7 Non-Photometric Nights—Differential Photometry . . . 9
- 2.8 Variable Stars . . . 10
  - 2.8.1 Intrinsic Variables . . . 10
  - 2.8.2 Extrinsic Variables . . . 12
- 2.9 The H-R Diagram . . . 13

3 Observations/Reductions **17**
- 3.1 CCDs and Calibration Frames . . . 17
- 3.2 Data Collection and Reduction . . . 18
- 3.3 IRAF . . . 21
- 3.4 VARSTAR . . . 21
- 3.5 Period04 . . . 22
- 3.6 Previous Research . . . 23
- 3.7 Methodology . . . 23

4 Data Analysis and Results **27**
- 4.1 Previously-Identified Variables . . . 27
  - 4.1.1 HD 205073 (Star 81 Short) . . . 27
  - 4.1.2 HD 205117 (Star 77 Short) . . . 29
  - 4.1.3 SAO 051002 (Star 72 Short) . . . 31

4.2 Potential Variables Observed 31
4.2.1 Star 10 Long 33
4.2.2 Star 24 Long / Star 2 Short 35
4.2.3 Star 25 Long 35
4.2.4 Star 57 Long 38
4.2.5 Star 58 Long 38
4.2.6 Star 90 Long 42
4.2.7 Star 96 Long / Star 25 Short 42
4.2.8 Star 111 Long / Star 28 Short 42
4.2.9 Star 143 Long / Star 40 Short 46
4.2.10 Star 147 Long 46
4.2.11 Star 163 Long 51
4.2.12 Star 164 Long 51
4.2.13 Star 184 Long 55
4.2.14 Star 222 Long 57
4.2.15 Star 42 Short 58
4.3 Conclusions and Future Research 58

Bibliography **60**

List of Figures

2.1 H-R Diagram 14

3.1 NGC 7092 Finder Chart 25

4.1 Light Curves for Star 81 Short (HD 205073). 28
4.2 Phased Light Curves for Star 81 Short 28
4.3 Light Curve for Star 77 Short (HD 205117) 29
4.4 Phased Light Curves for Star 77 Short 30
4.5 Light Curve for Star 72 Short (SAO 051002) 31
4.6 Phased Light Curves for Star 72 Short 32
4.7 Light Curves for Star 10 Long 33
4.8 Light Curves for Star 10 Long 33
4.9 Phased Light Curves for Star 10 Long 34
4.10 Light Curves for Star 24 Long 35
4.11 Phased Light Curves for Star 24 Long 36
4.12 Light Curve for Star 2 Short 36
4.13 Phased Light Curves for Star 2 Short 37
4.14 Light Curves for Star 25 Long 37
4.15 Phased Light Curves for Star 25 Long 38
4.16 Light Curves for Star 57 Long 39
4.17 Light Curve for Star 57 Long 39
4.18 Phased Light Curves for Star 57 Long 39
4.19 Light Curves for Star 58 Long 40
4.20 Light Curve for Star 58 Long 40
4.21 Phased Light Curves for Star 58 Long 41
4.22 Light Curve for Star 90 Long 42
4.23 Phased Light Curves for Star 90 Long 43
4.24 Light Curve for Star 96 Long 43
4.25 Phased Light Curves for Star 96 Long 44
4.26 Phased Light Curves for Star 25 Short 45
4.27 Light Curves for Star 111 Long 46
4.28 Phased Light Curves for Star 111 Long 47
4.29 Light Curve for Star 28 Short 47

4.30 Phased Light Curves for Star 28 Short 48
4.31 Light Curves for Star 143 Long 48
4.32 Light Curve for Star 143 Long 49
4.33 Phased Light Curves for Star 143 Long 49
4.34 Phased Light Curves for Star 40 Short 50
4.35 Light Curves for Star 147 Long 51
4.36 Phased Light Curves for Star 147 Long 52
4.37 Light Curves for Star 163 Long 52
4.38 Phased Light Curves for Star 163 Long 53
4.39 Light Curves for Star 164 Long 53
4.40 Light Curve for Star 164 Long 53
4.41 Phased Light Curves for Star 164 Long 54
4.42 Light Curves for Star 184 Long 55
4.43 Light Curve for Star 184 Long 55
4.44 Phased Light Curves for Star 184 Long 56
4.45 Light Curves for Star 222 Long 57
4.46 Light Curve for Star 222 Long 57
4.47 Phased Light Curves for Star 222 Long 58
4.48 Light Curves for Star 42 Short 59
4.49 Phased Light Curves for Star 42 Short 59

List of Tables

2.1 Pulsating Variable Types 11
2.2 Pulsating Variable Types, Cont. 11
2.3 Explosive/Eruptive Variable Types 11
2.4 Explosive/Eruptive Variable Types, Cont. 11
2.5 Non-Pulsating Variable Types 12

3.1 Table of Observations of NGC 7092 19
3.2 Table of CCDs 20
3.3 Table of Long-Exposure Magnitudes Observed 20
3.4 Table of Short-Exposure Magnitudes Observed 20
3.5 Equivalent Short and Long Stars Observed 24
3.6 Equivalent Short and Long Potential Variables 26

Chapter 1

Introduction

1.1 Why Astronomy

As an astronomer, people often interrogate me on what exactly a career in astronomy involves. The initial exclamation of interest ("Oh, you're an astronomer!") quickly trails off into, "So . . . what do you do, just look at stars all day?" The essence of such a question is actually very legitimate. Someone not familiar to the field would wonder what kind of useful information we could possibly glean from staring at far-away, seemingly out-of-reach bodies of light and gas and particles.

Even in their physically elusive natures—with the millions upon millions of light years of distance separating us from the most distant reaches of the universe—we are not immune to the consequences of these celestial objects' existence. The mysteries of the universe are intricately interwoven into our own way of life and progress. An ingredient to our very existence as living beings—the carbon in our bodies—is recycled stardust. Communication and weather satellites, radio, phone, and television are all directly linked to humans' efforts to reach out into space. Biology studied here on Earth is given greater dimension when compared to biological and climactic

samples found on other moons and planets, often providing key pieces to a puzzle that would have been unavailable on Earth. Medical advances and technology, transportation, communication—virtually all are linked in some way to mankind's commitment toward understanding the world, and worlds, around us.

As far as we know, the properties of physics are universal—consistent across space and time. The universe is an expanded mirror image of the way life exists right here on Earth; every aspect of matter mimics the movements of a vast pattern, reflecting right down to the motions of the smallest particle. In our own local solar neighborhood we only possess a small sampling of all the many extraterrestrial objects available to choose from, and only the tiniest window into all the aspects of stellar evolution, or the study of how stars change in time. Observing faraway bodies helps us to better perceive the role of our own sun in the universe, consequently giving us a greater understanding of answers to the old, classical questions of, "Could there be life elsewhere?" "How different can a planet be from what we know on earth and still sustain life as we know it?" "Where have we come from and where are we headed?" Though mere idle musings now, the answers to such questions could one day become quite significant.

1.2 Why Variable Stars

What we are studying in this thesis is a particular brand of stellar evolution: that of variable stars in the sparse open cluster NGC 7092 (more commonly known as M39), located in the constellation Cygnus. Open clusters such as this consist of groups of many thousands of stars that all formed in the same giant molecular cloud and are still loosely gravitationally bound to one another. These stars are physically related; born at the same time, they will share the same chemical composition, as well as the same

radial velocities, proper motions through space, age, and distance from Earth. This makes clusters very useful in the study of stellar evolution because they offer fixed parameters with which to make comparisons among the cluster's stars. Differences in stars' brightness, then, will be due mainly to differences in mass.

Variable stars consist of those that have become unstable at some point in their lifetime and now fluctuate in luminosity. Our goal is to search out and identify these in the hopes of launching future, in-depth research involving classification of the variation mechanism, eventually leading to a clearer understanding of the physics behind the stars themselves and their roles in stellar evolution.

1.3 Thesis Overview

This thesis will cover several topics of interest specific to variable stars. In the "Background" chapter, we will discuss the most basic and important concepts of astronomy. In "Observations/Reductions," data reduction methods will be described, along with research previously performed on M39 variables. In "Data Analysis and Results," we outline our own potential variable star discoveries and their light curves, phase diagrams, and periods. In the "Conclusions" section we will summarize our research and point out possibilities for future projects.

Chapter 2

Background

2.1 HJD

Because astronomy is a globally-studied science and very dependent on time values, a standardized time system needs to be implemented to keep the data uniform. Astronomers have decided on the Heliocentric Julian date (HJD) as the standard. The Julian Date is defined as the number of days that have elapsed since noon of Monday, January 1st, 4713 BC in Greenwich, England, the zeropoint of observational time. However, astronomers must also take into account the fact that from the point of view of an observer on Earth, the time it takes the light of an object to reach that observer varies according to the seasons—how the earth is tilted in regards to the sun during any particular time of the year. This requires all of time to be moved to a heliocentric, or sun-centered, centerpoint. With the resulting value, easily calculable in data reduction programs, astronomy can standardize its data to a common time.

2.2 Light Curves

A light curve is a graph of a celestial body's light intensity as a function of time (HJD)—it shows how its brightness acts during an observation. Light curves can be used to derive periods, estimate rotation rates, classify brightness variations, and generate information about the processes that produce them. Light curves are extremely useful in identifying variable stars. Examination of their shapes are crucial in differentiating variable classes.

2.3 The Magnitude Scale

When Hipparchus, an early astronomer living in 190 BC Greece, surveyed the night sky, he perceived that the night's assortment of stars appeared to vary over a noticeable range of brightness. He eventually developed a scale to account for these differences, covering five steps in magnitude—1st magnitude representing the brightest stars, and 6th representing the dimmest. Today's astronomers, blessed with greater technology and the advantage of high-quality telescopes both on the earth's surface and outside its atmosphere, have quantified the measurements mathematically, extending the scale to include extremely bright objects such as the sun (-26 magnitudes) and bodies so faint they are invisible to the naked eye at magnitudes of 7 or more. This scale takes into account the fact that the human eye is logarithmic in response, meaning that each magnitude the eye detects is twice as bright (or dim) as the following (or subsequent) iteration.

Due to the effects of distance and fluctuation in the atmosphere, magnitude must be further specified into two classes—absolute and apparent. Apparent magnitude is defined as how bright a celestial body appears to an observer on the earth. Apparent magnitudes must be normalized to the value they would have outside the atmosphere.

This is accomplished using the equation $m = -2.5\log_{10}(F) + C$, where F represents flux and C the zeropoint constant. The value obtained from this equation is also known as the instrumental apparent magnitude.

Absolute magnitude, on the other hand, defines itself as the apparent magnitude an object would have in the absence of atmospheric extinction and if it were at a standard luminosity distance away from us, the observers. In other words, it allows the brightness of celestial bodies to be compared without regard to distance. The equation for absolute magnitude is represented as $m-M = 5\log_{10}(d)-5$, where $m-M$ symbolizes the distance modulus (apparent magnitude minus absolute magnitude), and we are defining magnitudes at a standard distance of 10 parsecs.

2.4 Color

The term "color," in general, refers to how human eyes interact with various parts of the visible light spectrum (400-700 nm). Each color represents a different chunk of wavelength. In astronomy, we measure the difference in magnitude, or intensity, between two different filters at two separate wavelengths in order to define color. Filters are designed to examine specific regions of a star's blackbody curve; stated another way, they block light from all wavelengths except their target range. In our own data acquisition, involving the Johnson B, V, and R filters, the B−V (blue minus green) color index refers to the magnitude of the V filter subtracted from the B filter, and V−R (green minus red) represents the R filter subtracted from the V. This gives us our color index, where the long wavelength magnitude is subtracted from the short and the index is independent of distance.

2.5 Airmass/Extinction

As was discussed before, apparent magnitude is affected by variations in the Earth's atmosphere. This effect is called atmospheric extinction, or seeing. As it passes through the atmosphere, light is scattered and absorbed; the more atmosphere through which it passes, the greater this effect. By the time light hits the CCD, each wave emitted by the star has diverged in slightly different directions from their original paths, forming a skewed and dimmer image. For this reason, airmass—a light source's optical path length through Earth's atmosphere—is an important factor to take into account both in all-sky and differential photometry. Airmass measured at the zenith is 1 and increases with the angle between the zenith and the horizon, as extinction effects are greater at lower altitudes. This effect can then be plotted in terms of magnitude and subtracted from the observation.

2.6 Photometric Nights—All-Sky Photometry

Many different factors will influence the magnitudes of the stars we observe: plate scale, field crowding, airmass, filters used, color terms, cosmic ray hits, and exposure times, to name a few. On a photometric night, however, only a few of these effects will need to be corrected for. A photometric sky, or all-sky photometry, is characterized by a completely clear night free of clouds and haze, with stable seeing conditions and an observing time as near to the new moon as possible. We should be able to assume that the sky, for the most part, is uniform. In order to obtain good data on a photometric night, a standard field of known stable stars with which to calibrate our observations must first be selected. The observer will move the telescope back and forth between the standard field and the target object throughout the night, comparing observed values with those already known and using them to convert the

instrumental magnitudes to standard. Next, extinction correction must be performed. This is achieved by collecting data over a large airmass range. On a photometric night we have more freedom regarding the method of filter sequence we use. For example, some M39 data presented in this thesis was taken in a palindrome sequence—one set of observations is represented by the set B V R R V B. This gives a set of B, B−V, and V−R color indices for each observation. In this way we can compare the first and last B frames, ensuring that they are close in value and there are no errors.

2.7 Non-Photometric Nights—Differential Photometry

Some nighttime conditions, however, are not as ideal as we would like. In these instances we correct our data using differential photometry. CCDs, which will be more thoroughly defined in Section 3.1, are advantageous for non-photometric nights in the fact that they can see multiple stars at once and record sky brightness along with the image. With a single CCD frame we can assume our stars are of similar brightness. Differential photometry is then performed on a frame-by-frame basis by selecting an ensemble of non-varying stars from our observing field, averaging them, and subtracting them from our suspected variables. This process should effectively remove atmospheric fluctuations from our observations.

2.8 Variable Stars

2.8.1 Intrinsic Variables

Most stars, at some point in their lives, will experience a season of immense and rapid change. Some of these changes will occur in the star's atmosphere, others deep within the core of the star itself. The latter are called intrinsic variables because the makeup of the star itself is physically changing. Of the intrinsic variables, there are two main categories: pulsating and cataclysmic/eruptive. Pulsating consist of those that demonstrate periodic expansion and contraction of their surfaces, either radially or non-radially. The pulsating mechanism of a star is born when low mass, Population II (old with low metallicity) stars enter the instability strip on the HR diagram during their core helium-burning phase. At this stage of evolution, the star loses its hydrostatic equilibrium, meaning that the force of gravity acting on the outside surface fails to balance with the pressure on the inside. The star will then attempt to regulate itself by bringing itself back to hydrostatic equilibrium but, like an out-of-control pendulum, keeps overshooting—causing it to expand and contract between the extremes on either side of equilibrium until it has moved past the instability strip and onto a further stage of its evolution. Two thirds of all variable stars are predicted to be pulsating. If their magnitudes were to be plotted in time, they would be characterized by a smooth, sinuous curve.

Another type of intrinsic variable consists of the cataclysmic variable. Cataclysmic variables vary in brightness due to the violent processes taking place in their outer atmospheres. They demonstrate outbursts caused by thermonuclear processes occurring either in their surface layers or deep within their interiors. Astronomers term these violent explosions of activity "novae" or "supernovae." An outline of these relationships can be viewed in Tables 2.1-5 [4].

Table 2.1. Pulsating Variable Types

Type	*Absolute Magnitude (M)*	*Spectral Class*	*Average Period*
Cepheid	-0.5 to -0.6	F6 to K2	5 to 10 days
RR Lyrae	0.5 to 1	A2 to F6	0.5 days
RV Tauri	0 to -3	G, K	75 days
Mira	1 to -2	M1 to M6	270 days

Table 2.2. Pulsating Variable Types, Cont.

Type	*Description*
Cepheid	Pop I yellow giants, 3-18 solar masses,cross upper region of instability strip during core He burning
RR Lyrae	Low mass Pop II stars, standard candles,traverse instability strip during core He burning
RV Tauri	Yellow supergiants, irregular
Mira	Red giants, long periods, late stages of evolution

Table 2.3. Explosive/Eruptive Variable Types

Type	*Maximum Magnitude (M)*	*Energy Per Eruption (J)*	*Total Magnitude Change (M)*
Novae	-5.5 to -9.2	6×10^{37}	8 to 13
Dwarf Novae	5.5	6×10^{31}	4
Supernovae	-18 to -20	10^{43} to 10^{44}	Greater than 20

Table 2.4. Explosive/Eruptive Variable Types, Cont.

Type	*Description*
Novae	Result from fusion and subsequent explosion of hydrogen
Dwarf Novae	Result from instability in accretion disc
Supernovae	Result from cessation of fusion and gravitational collapse

Table 2.5. Non-Pulsating Variable Types

Type	*Description*
Flare Stars	Pre main-sequence, solar mass, exhibit flaring activity
T-Tauri Stars	Pre main-sequence, low solar mass, spectroscopically active, fluctuate rapidly in X-rays
Spectrum Variables	Exhibit variable spectra
Magnetic Stars	In later phase of evolution, possess variable magnetic fields

2.8.2 Extrinsic Variables

Extrinsic variables are related to how we view things from Earth. When the moon passes in its orbit between us here on Earth and the sun, we are seeing a solar eclipse—part of the sun's light will be blocked out due to the moon obstructing our line of sight. The sun itself, however, is not actually varying in luminosity or temperature. This is how we classify eclipsing variables—two stars making up a binary system eclipsing each other as they rotate around one another. Such binary systems make up at least half the stars in the sky. Because they are so far away, each star individually is generally unresolvable with a telescope—meaning they would appear on a computer screen simply as a single pixellated blur of light. However, their light curves can tell us much. If we were to discover an eclipsing variable in M39, its light curve would appear to be generally flat with sudden drops characterizing the moment of eclipse. This curve will actually represent the magnitude changes of both stars combined, varying somewhat according to the size of the system's stars relative to each other.

Rotating variables make up the other type of extrinsic variability; these appear variable to an observer on Earth due to their axial rotation. For example—not all celestial bodies are perfectly spherical; some, such as asteroids, are quite ellipsoidal. Irregular shapes such as these present different portions of surface area to an observer

on Earth as they rotate, creating irregular and varied light curves. Other phenomena, such as sunspots or other chemical or thermal inhomogeneity, conceive similar variations in the light curves.

As the data in this study covers long periods of the night over a range of several nights, we hope to uncover stars exhibiting several of the light curve types listed above. In studying variables ranging through many different moments of a star's life cycle, we can further our knowledge and understanding of stellar evolution in general.

2.9 The H-R Diagram

A Hertzsprung-Russell (H-R) diagram illustrations relationships among stars according to their spectral classes by plotting magnitude versus spectral type, or the equivalent to luminosity versus temperature (see Fig. 2.1). Brightness and color depend on surface temperature, which in turn depends on the star's mass; spectral classes group stars by the relative strengths of the spectral lines they emit. Where a star lies on this plot reveals the state of its evolution. For example, younger to middle-aged stars, still fusing hydrogen in their cores, lie along the main sequence line. Following this stage are the horizontal and red giant branches, whose stars sustain masses similar to that of our sun's. The instability strip represents a nearly vertical region intersecting the main sequence in the A-F classes and climbing toward the highest luminosities. Stars in this area, undergoing a doubly-ionized helium phase, are expanding and contracting due to changes in density, temperature, and opacity: this is the region occupied by pulsating variables, or stars that undergo physical changes as their compositions are altered through thermonuclear reactions.

H-R diagrams are incredibly useful in learning more about stellar evolution: matching plots of our own observed stars with theoretical groups on the H-R diagram can

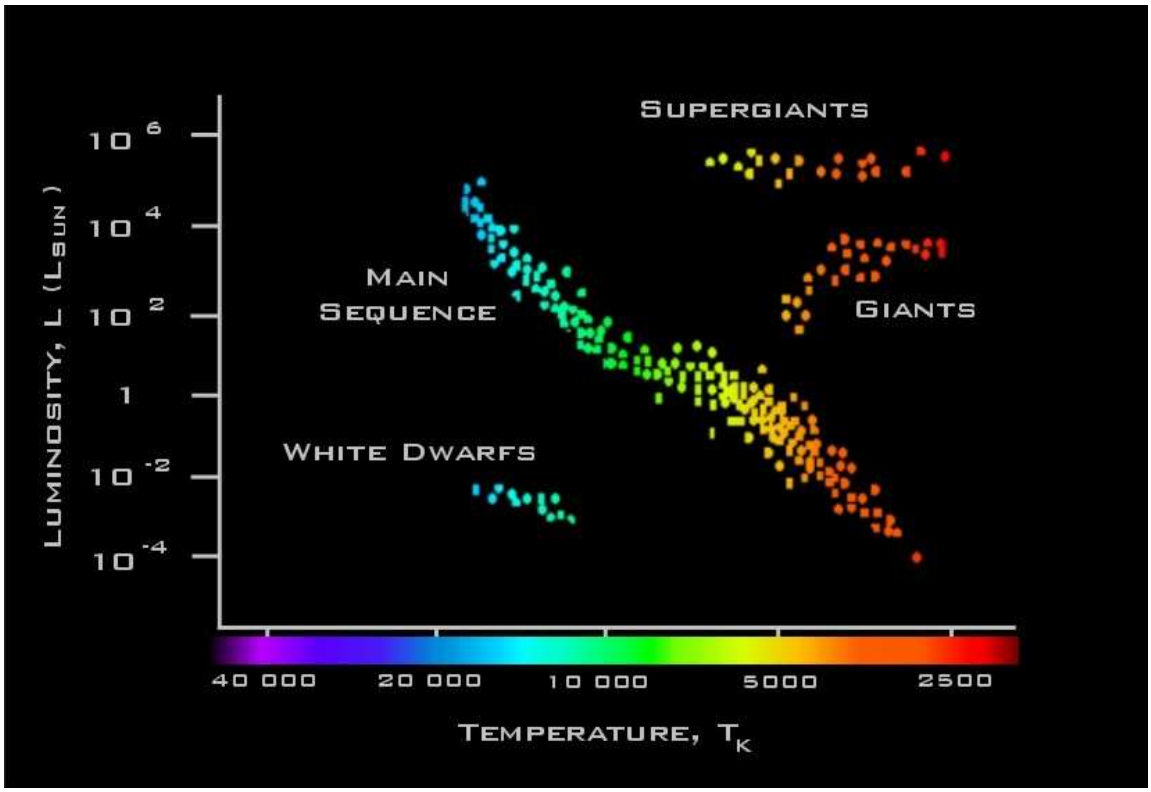

Figure 2.1 Example of an H-R Diagram. Image taken from *http : www.le.ac.uk/ph/faulkes/web/images/hrcolour.jpg*

give us much insight into the expanse of our stars' extended lifetimes.

Chapter 3

Observations/Reductions

3.1 CCDs and Calibration Frames

We use CCDs, or charge-coupled devices, to capture digital images and record data on multiple stars at a time. Unlike its predecessors, photographic plates and photo-multiplier tubes, the CCD exhibits 70 to 95% quantum efficiency. This means that it has a high ratio of the number of photons detected compared to the total number received. A CCD contains a grid of pixels acting as photon-counters. When a photon hits this array of light-sensitive pixels, it is transformed into an electron-hole pair by the CCD's underlying semiconductors. Electrical charge proportional to the light intensity of each star in the field is then built up in each corresponding location of detected light, effectively creating a grid of electron "wells." Once the exposure is stopped, electrons can be counted and converted into digital memory accessible as computer images.

Before CCD-collected data can be used, however, it must first be reduced. Thermal noise and dark current, as well as fluctuations of the electronics and amplifiers, can alter pixels in a CCD array. These cause extra electrons to be placed in the

"wells," making their counts disproportionate to the amount of photons originally detected from the star source. Data must therefore be standardized before it can be processed. This is done partially with calibration frames. A "bias" or "zero" frame is a zero-length exposure. Each pixel has a slightly different zero level; therefore, the bias frame must be subtracted from each object frame, or image. A dark frame is an exposure taken with the camera shutter closed and should be proportional to the length of the object exposures. As with the bias frames, when current is applied to the CCD array extra electrons can sometimes fall into the "wells." Each pixel may respond differently to this dark current; likewise, the dark frames must be subtracted. Bias and dark frames both take advantage of the fact that certain components of image noise are the same in every frame. Generally several of each of these bias and dark frames are combined into sets and averaged before they are subtracted in order to minimize errors or random fluctuations in any single frame, and to reduce image noise in regions of low signal level. Lastly, flat fields are taken by aiming the detector at a surface with a uniform brightness over the entire area, such as a screen or the dawn and twilight skies. Instead of being subtracted, these flats are scaled to an average of 1 and divided through the object frames.

3.2 Data Collection and Reduction

Our data were collected largely using the 0.4 m David Derrick Telescope (DDT) of the Orson Pratt Observatory of Brigham Young University. Data taken in 2005 employed a Cassegrain mounted with an SBIG ST-1001 CCD of plate scale 0.98 arcsec/pixel, pixel size 24 μm, and 1024 x 1024 array size. Data in 2004 were collected on an Apogee Ap47p CCD with a 1.32 arcsec/pixel plate scale, 13μm pixel size, and 1056 x 1024 array size. One night of data, 5 Aug. 2006, was taken with the West Mount 0.3

Table 3.1. Table of Observations of NGC 7092

Date (UT)	*Observatory*	*Telescope*	*CCD Used*	*V exp. (s)*	*Number of Frames*
14 September 2004	OPO	DDT 0.4 m	Apogee Ap47p	120,8	15
2 November 2004	OPO	DDT 0.4 m	Apogee Ap47p	10	225
15 October 2005	OPO	DDT 0.4 m	SBIG ST-1001	40,8	6
23 November 2005	OPO	DDT 0.4 m	SBIG ST-1001	100,5	64
5 August 2006	WMO	WMT 0.3 m	SBIG ST-1001	30	200

m telescope (WMT), with an ST-1001 CCD with pixel size and focal ratio identical to the DDT's ST-1001 and an array size of 1092x736. The data yielded by this telescope are their own topic of interest, as the summer of 2006 served as its maiden voyage during which several kinks still needed to be worked out of our observations. Also needing to be taken into account, however, are the photometric conditions, which are much clearer at West Mount than BYU campus. We mention this as an item of note when considering all data presented here from the night of 5 Aug. 2006, and as a possible subject of future research. A comparison chart of a selection of random stars and their observed differential magnitudes for each night, including those of 5 Aug. 2006 from West Mount, is shown in Tables 3.3-4. This data shows that every night is photometrically consistent between observatories and exposure lengths, at least in terms of differential magnitude, and doesn't seem to demonstrate any photometric advantage from West Mount's 0.3 m during its first summer. A comparison of CCDs can be found in Table 3.2.

All data were collected using standard Johnson B, V, and R filters; however, only the results of the V (central wavelength 5500 Å) are listed here. A table of exposure times in the V filter is presented in Table 3.1.

Table 3.2. Table of CCDs

Observatory	*CCD*	*Focal Ratio*	*Plate Scale*	*Pixel Size*	*Array Size*
OPO	Apogee Ap47p	f/16	1.32 arcsec/pixel	13.6 μm	1056 x 1024 pixels
OPO	SBIG ST-1001	f/16	0.98 arcsec/pixel	24 μm	1024 x 1024 pixels
WMO	SBIG ST-10	f/12.5	0.98 arcsec/pixel	13.6 μm	1092 x 736 pixels

Table 3.3. Table of Long-Exposure Magnitudes Observed

Object	14 *Sept.* 2004 (M)	23 *Nov.* 2005 M)	15 *Oct.* 2005 (M)	5 *Aug.* 2006 (M)
Star 24 Long	13.19	14.01	13.86	13.57
Star 52 Long	9.15	10.02	9.91	9.69
Star 62 Long	13.24	14.22	14.06	13.84
Star 72 Long	12.83	13.72	13.53	13.38
Star 77 Long	12.97	14.09	14.62	13.65
Star 86 Long	13.91	14.74	14.59	14.32
Star 96 Long	13.03	13.85	13.72	13.48

Table 3.4. Table of Short-Exposure Magnitudes Observed

Object	14 *Sept.* 2004 (M)	23 *Nov.* 2005 (M)	15 *Oct.* 2005 (M)	5 *Aug.* 2006 (M)
Star 2 Short	13.21	13.18	14.03	13.92
Star 10 Short	9.23	9.22	9.91	10.10
Star 13 Short	13.32	13.27	14.13	14.22
Star 15 Short	12.88	12.87	13.44	13.65
Star 18 Short	12.96	12.94	14.32	14.70
Star 20 Short	13.82	13.86	14.46	14.42
Star 25 Short	13.06	13.05	13.70	13.90

3.3 IRAF

Raw data were processed in IRAF (Image Reduction and Analysis Facility), an expansive set of programs compiled by astronomers for analysis and reduction of photometric or spectroscopic data. We used IRAF to first combine and subtract the bias frames from our dark frames. We then performed a similar procedure on our darks, combining them and then using them to zero- and dark-correct our flat field. The flats were subsequently combined and applied to our object frames, resulting in fully-calibrated images that could then yield magnitudal data.

3.4 VARSTAR

Once the object frames have been calibrated, we can measure the instrumental magnitudes of our stars in the frame, after which the output files of the measured magnitudes are separated into groups. A collection of "stable" stars—those with lower error per observation averages—are collected to create an ensemble that will then be averaged and subtracted from the instrumental magnitude of each star measured. Stars with higher errors of magnitude represent potential variables because their magnitudes are constantly changing; these need to be removed from the average in order to create a stable ensemble. The aforementioned ensemble is finally perfected by repeatedly rerunning the sequence of information, removing any stars with high error of magnitude each time until it becomes a group constituted of the highest stability possible. This entire process is performed in the IRAF package VARSTAR5, written by Dr. Eric Hintz of Brigham Young University. After processing the data with the stable ensemble, it will output magnitude versus HJD files for each star we collected data for. These numbers can then be plotted and used to either establish periods of previously-known variables or discover new variables altogether. Another method

of detecting potential variables through VARSTAR5 involves plotting error versus magnitude of only the ensemble members altogether on one plot and fitting it to a logarithmic curve. This approach seemed to work best on near-photometric nights. Examining the plot, we see an error curve that is flat at low (bright) magnitudes but increases with differential magnitude value. This is to be expected, as noise increases and signal decreases at fainter magnitudes. Stars that lie significantly above the error line often represent potential variables. We can then examine the light curves of each of these potentials, determining whether they are, in fact, variables or simply very noisy stars. In our research we employed both the error versus magnitude and magnitude versus HJD methods of variable detection. Due to the general status of our nights, however, most of which were not quite photometric, the magnitude versus HJD light curves were predominately considered in the analysis of the final data.

3.5 Period04

Once all the data from each night have been collected, reduced, and represented as light curves, they will need to be run through a Fourier analysis in order for a period to be obtained. On occasion, a star will exhibit slightly different amplitudes in each cycle, oftentimes because it is multiperiodic. Overtones and beat terms may also contribute, sometimes greatly complicating the apparent light curve. For this reason, we must discover which frequencies actually add to the overall shape by extracting one cycle at a time and fitting sine curves to the data. We do this by determining the most dominant sine wave and then subtracting its fit from the data. We repeat this process with the next wave, and continue until we hit noise level. We used Period04, a program written by Martin Sperle, for this analysis [5]. Once we have obtained an overall fit, each night's data can be phased into one single light curve. This will help

us further determine the variability of our stars.

3.6 Previous Research

The General Catalogue of Variable Stars (GCVS) [6] lists three stars within our field of data that demonstrate some form of variation: HD 205073 (α=$21^h31^m23^s$, δ=+48° 21'25"); HD 205117 (α=$21^h31^m44.7^s$, δ=+48° 29'04"); and SAO 051002 (α=$21^h32^m18.5^s$, δ=+48° 20'32"), J2000. These correspond, respectively, to our arbitrarily-numbered suspected variables, Stars 81 Short, 77 Short, and 72 Short. These stars are examined more closely in the Data Analysis and Results chapter.

3.7 Methodology

The purpose of this research was to examine M39, figuratively, both on the inside and out. In other words, we wanted to investigate the bright, well-studied giants, but hoped to delve deeper into the realm of the fainter, generally overlooked stars as well. This required two sets of exposure times: short and long (see Fig. 3.1). The short exposure times varied between 5 and 8 seconds and allowed us to examine a set of 81 of M39's brighter members without risking oversaturation. The long exposure times ranged from 30 to 120 seconds and collected the light of 228 stars, some reaching magnitudes as faint as 20. Between the two sets of data, 72 stars overlapped, meaning we obtained data in both long and short exposures for these. Of the long set, 14 are suspected to be variable, whereas five are suspected of the short. Four of these are found in both sets, making 15 potential variables altogether with new data. The three previously-discovered variables were observed only in the short. Furthermore, all nights were taken in V filters in both sets of exposures. These relationships are

Table 3.5. Equivalent Short and Long Stars Observed

Short Exp.	*Long Exp.*	*Short Exp.*	*Long Exp.*	*Short Exp.*	*Long Exp.*
Star 1	Star 22	Star 31	Star 122	Star 61	Star 206
Star 2	Star 24	Star 32	Star 128	Star 62	Star 208
Star 3	Star 26	Star 33	Star 129	Star 63	Star 209
Star 4	Star 27	Star 34	Star 130	Star 64	Star 211
Star 5	Star 34	Star 35	Star 131	Star 65	Star 214
Star 6	Star 35	Star 36	Star 135	Star 66	Star 215
Star 7	Star 37	Star 37	Star 136	Star 67	Star 217
Star 8	Star 46	Star 38	Star 140	Star 68	Star 218
Star 9	Star 47	Star 39	Star 142	Star 69	Star 219
Star 10	Star 52	Star 40	Star 143	Star 70	Star 220
Star 11	Star 54	Star 41	Star 144	Star 61	Star 206
Star 12	Star 55	Star 42	Star 149	Star 71	Star 228
Star 13	Star 62	Star 43	Star 153	Star 72	N/A
Star 14	Star 69	Star 44	Star 168	Star 73	N/A
Star 15	Star 72	Star 45	Star 171	Star 74	N/A
Star 16	Star 73	Star 46	Star 172	Star 75	N/A
Star 17	Star 76	Star 47	Star 173	Star 76	N/A
Star 18	Star 77	Star 48	Star 175	Star 77	N/A
Star 19	Star 85	Star 49	Star 178	Star 78	Star 156
Star 20	Star 86	Star 50	Star 182	Star 79	N/A
Star 21	Star 87	Star 51	Star 187	Star 80	N/A
Star 22	Star 88	Star 52	Star 188	Star 81	N/A
Star 23	Star 93	Star 53	Star 190	...	...
Star 24	Star 94	Star 54	Star 193	...	...
Star 25	Star 96	Star 55	Star 194	...	...
Star 26	Star 102	Star 56	Star 200	...	...
Star 27	Star 108	Star 57	Star 202	...	...
Star 28	Star 111	Star 58	Star 203	...	...
Star 29	Star 119	Star 59	Star 204	...	...
Star 30	Star 120	Star 60	Star 205	...	...

all illustrated in Tables 3.5-6.

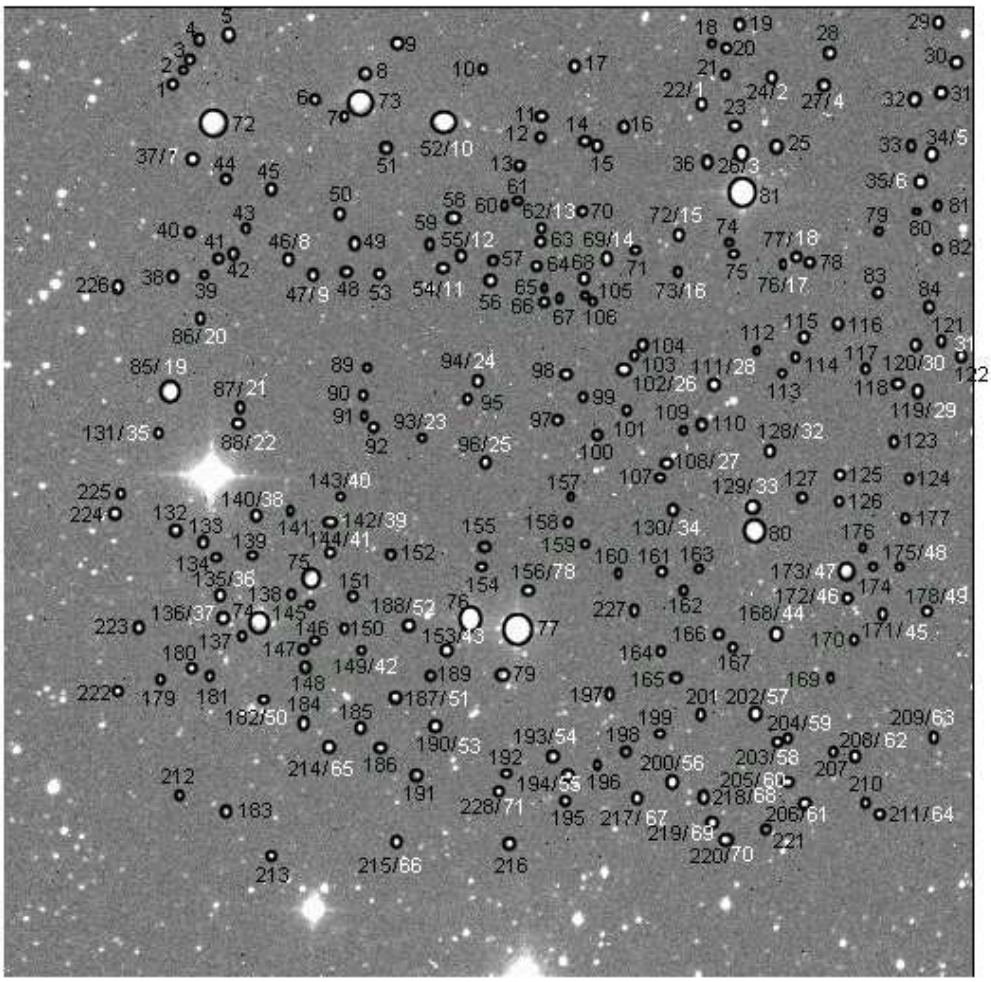

Figure 3.1 NGC 7092 finder chart. Stars observed in long exposures are labeled in black; short exposures are labeled in white. Numbering was chosen arbitrarily.

Table 3.6. Equivalent Short and Long Potential Variables

Short Potentials	*Long Potentials*
...	Star 10
Star 2	Star 24
...	Star 25
...	Star 57
...	Star 58
...	Star 90
Star 25	Star 96
Star 28	Star 111
Star 40	Star 143
...	Star 147
...	Star 163
...	Star 164
...	Star 184
...	Star 222
Star 72	...
Star 77	...
Star 81	...

Chapter 4

Data Analysis and Results

4.1 Previously-Identified Variables

4.1.1 HD 205073 (Star 81 Short)

In his Geneva Observatory Star Catalogue, F. Rufener finds HD 205073 to be variable with an average magnitude of 7.85 [7]. The American Association of Variable Star Observers lists an official range of 7.66 to 7.85 magnitudes [8]. Its spectral type is described as $A\,m$, whereas Rufener labels it as a type $A0\,Vs$. Other than describing it as having an "abnormal disperson, particularly in U and G colors," no information about this star's period is listed in the literature.

Our own observations yielded a period of 0.090412 days, or about 2.2 hours. One of the brighter members of our study, Star 81 Short ranged over a total magnitude change of roughly 0.05 from peak to peak. Light curves from two separate nights show what appears to be a constant, sinusoidal period, as does Star 81 Short's phase diagram. These are shown in Fig. 4.1-2.

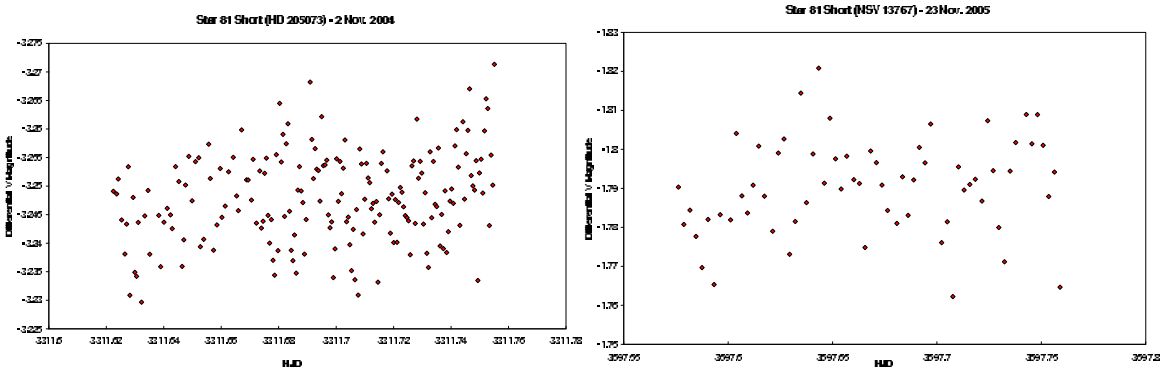

Figure 4.1 Light Curves for Star 81 Short (HD 205073), taken 2 Nov. 2004 and 23 Nov. 2005

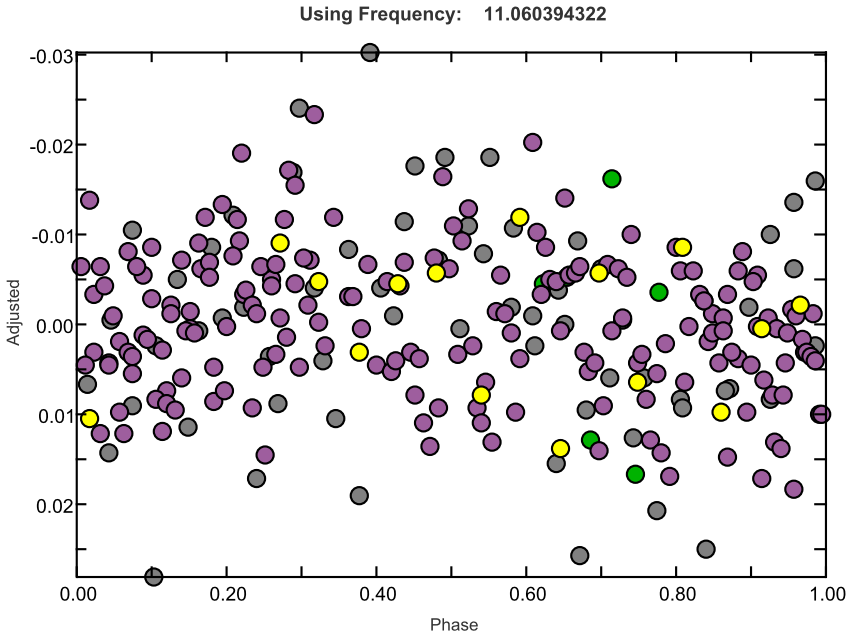

Figure 4.2 Phased Light Curves of Four Nights for Star 81 Short. Observed Phase Period: 0.09^d.

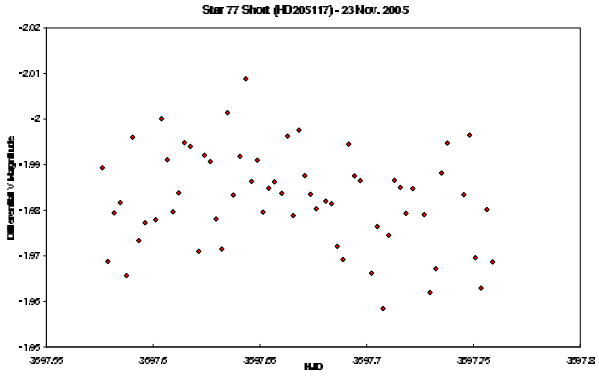

Figure 4.3 Light Curve for Star 77 Short (HD 205117), taken 23 Nov. 2005.

4.1.2 HD 205117 (Star 77 Short)

HD 205117, the most studied of our three previously-observed variables, was found by Zakirov, Arzumanyants, and Ishakulov to exhibit magnitudes ranging from 7.69 to 7.77 [9]. While the General Catalogue of Variable Stars lists its spectral type as $A0\ IV$, Rufener pins it as a type $A0\ Vs$ [7]. According to Zakirov et. al. [9], it is a probable binary, with each component existing as a subgiant. Zakirov et. al. also listed a real period of 113.2 days, making it a much longer-range star than what this study covers. Our own research found a period of only 0.189624 days, or about 4.5 hours. This period was most noticeable in the light curve for 23 November 2005, which demonstrates apparent sinusoidal motion. When phased with the other three nights, however, the variable motion disappears somewhat—albeit some rise in the curve can still be picked out. More study is needed to resolve these discrepancies, both between the previously-observed period and our own, as well as our one night's light curve compared to the others. Diagrams are shown in Fig. 4.3-4.

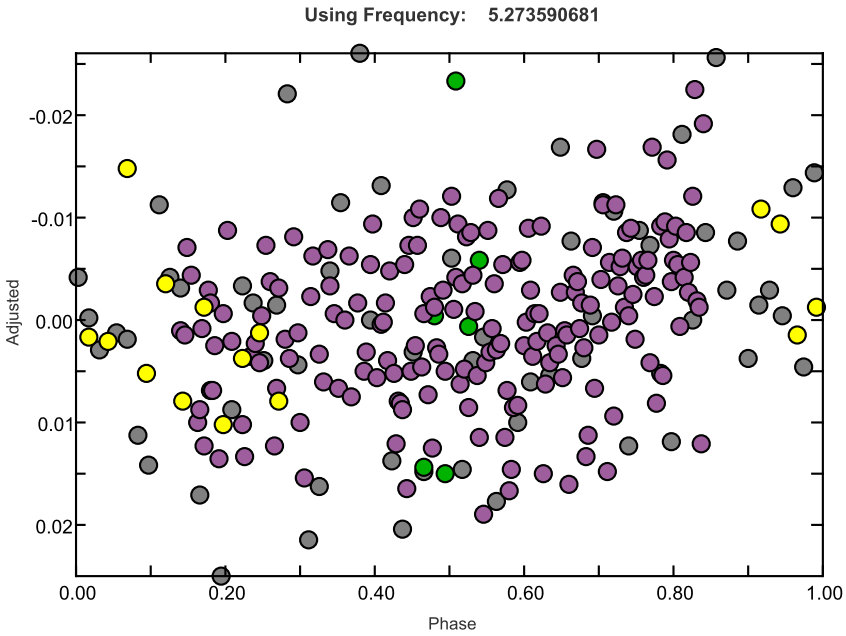

Figure 4.4 Phased Light Curves of Four Nights for Star 77 Short. Observed Phase Period: 0.189^d.

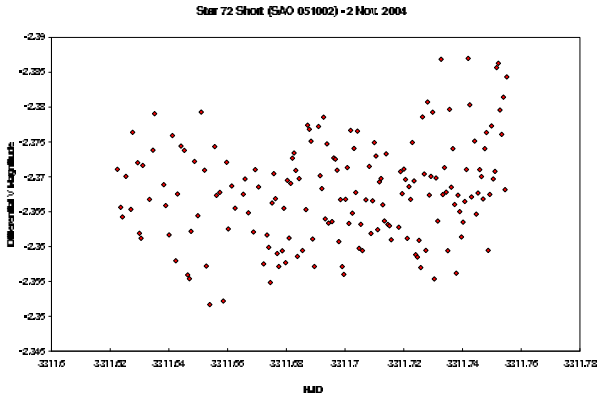

Figure 4.5 Light Curve for Star 72 Short (SAO 051002), taken 2 Nov. 2004.

4.1.3 SAO 051002 (Star 72 Short)

As obtained from the AAVSO website, SAO 051002 demonstrates an average magnitude of 8.69 with a spectral type of *AI V* [8]. Rufener, in a publication ten years later, describes it as microvariable in color, though no official period was listed [10]. Our research uncovers a very brief period of 0.0264925 days, or about half an hour—the most rapidly varying of the three. As can be seen in Fig. 4.5-6, a distinct periodic variation exists.

4.2 Potential Variables Observed

Of the 15 total candidates, 10 stars lie exclusively in the long exposure group, while four will compare data from both short and long exposures (see Table 3.6). Several stars from the night of 5 Aug. 2006 were left out altogether, as the West Mount 0.3 m CCD was operating on an oddly-shaped 1092x736 array size. Two other stars, 27 and 42 Short, hail from the short group only, though both demonstrate apparent variation on one or two nights only and fail to phase well. One star from the long group, 147 Long, exhibits similar messy behavior. All will still be listed, however,

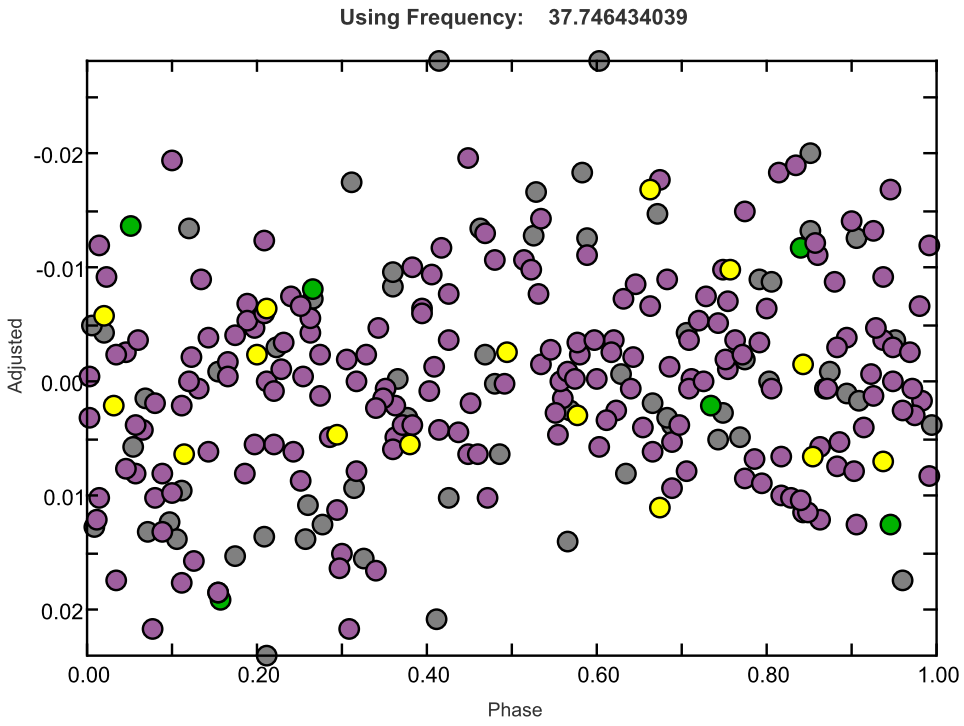

Figure 4.6 Phased Light Curves of Four Nights for Star 72 Short. Observed Phase Period: 0.026^d.

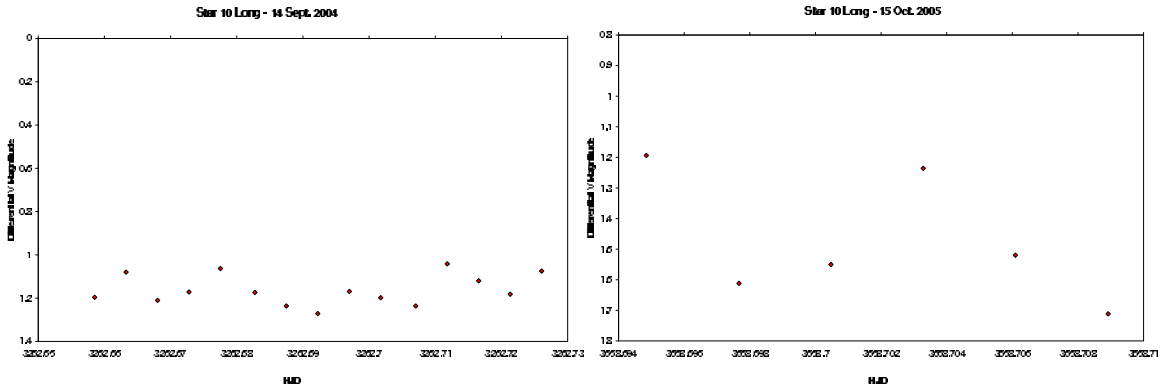

Figure 4.7 Light Curves for Star 10 Long, taken 14 Sept. 2004 and 15 Oct. 2005.

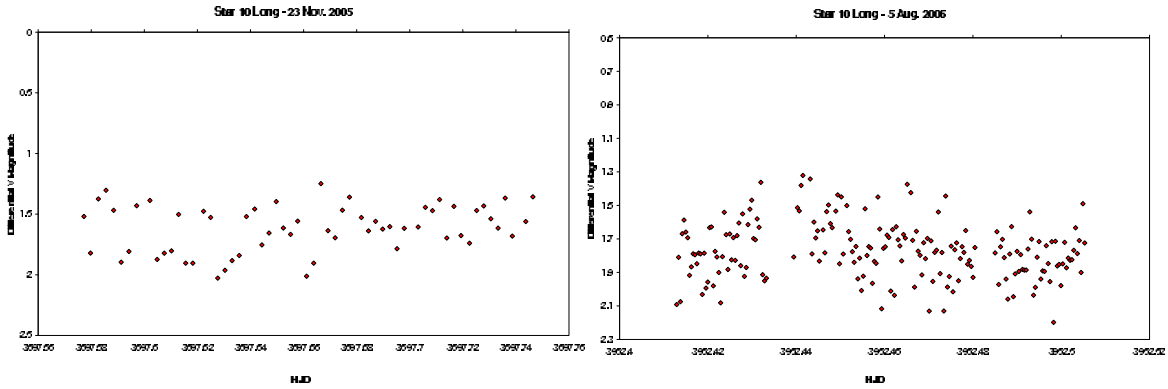

Figure 4.8 Light Curves for Star 10 Long, taken 23 Nov. 2005 and 5 Aug. 2006.

in pursuit of creating a foundation for further future study. All observed candidates ranged in period from 0.02 to 0.15 days.

4.2.1 Star 10 Long

In light curves from 2004 and 2005, Star 10 Long exhibits tiny, rapid variations, while the light curve for 5 Aug 2006 peaks early in the night and then flattens out somewhat. When phased, however, this star seems to smooth out into a regular, gentle rise and fall with an observed period of 0.081038 days (almost 2 hours). (See Fig. 4.7-9.)

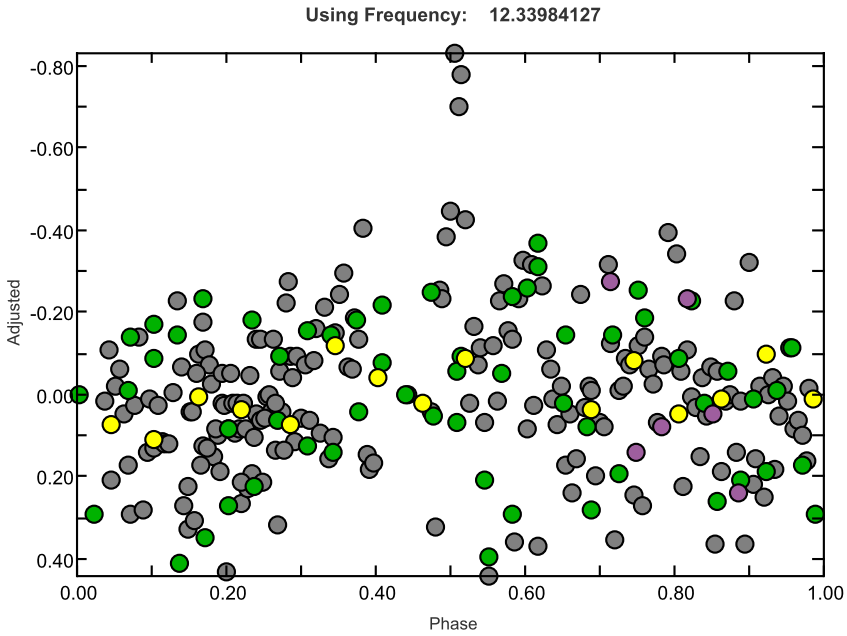

Figure 4.9 Phased Light Curves of Four Nights for Star 10 Long. Observed Phase Period: 0.028^d.

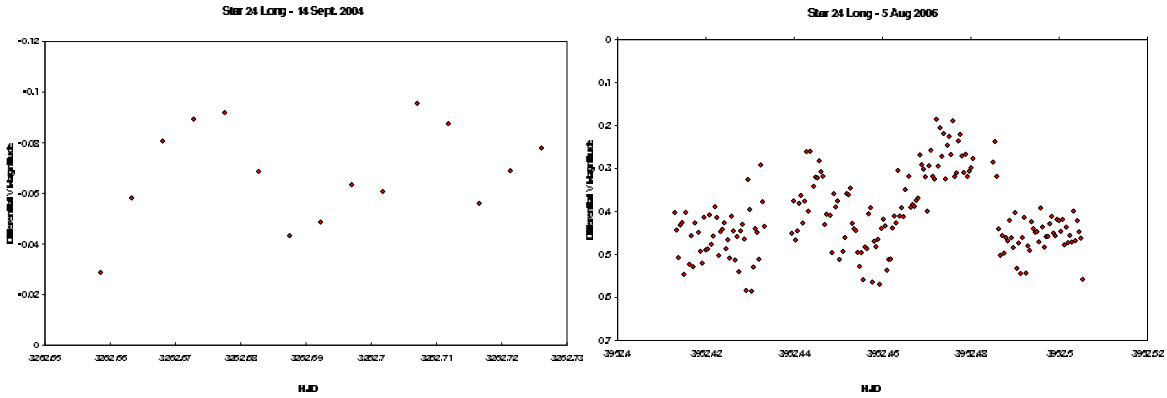

Figure 4.10 Light Curves for Star 24 Long, taken 14 Sept. 2004 and 5 Aug 2006.

4.2.2 Star 24 Long / Star 2 Short

Stars 24 Long and 2 Short, although the same star observed at different exposure times, were observed with different periods. Star 24 Long derives a calculated period of 0.035912 (about 51 minutes), while the period for Star 2 Short was predicted at an unusually low 0.0029 days. Furthermore, light curves of 24 Long demonstrate distinct variability while those for 2 Short seem solidly stable. These discrepancies could be due to any number of reasons: bad data, less-than-photometric nights, or a misnumbering in the comparison between the long and short fields, among others. For now, we will assume variability of 24 Long at its 0.0029 day period until the legitimacy of 2 Short can be procured in future research. (See Fig. 4.10-13.)

4.2.3 Star 25 Long

Star 25 Long exhibited enough nights of variable activity to classify it as a suspected variable. When phased, however, its period fell suspiciously low at 0.02 days. We therefore re-phased our data, excluding two nights of "bad" light curves. This time around we obtained a period of 0.115009 days (2.76 hours), which seemed much more reasonable. (See Fig. 4.14-15.)

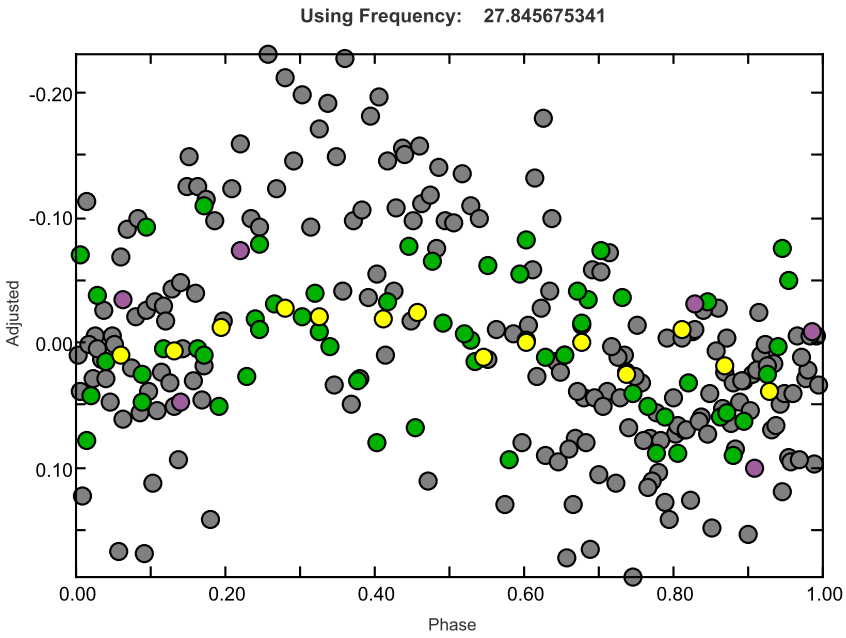

Figure 4.11 Phased Light Curves of Four Nights for Star 24 Long. Observed phase periods: 0.036^d.

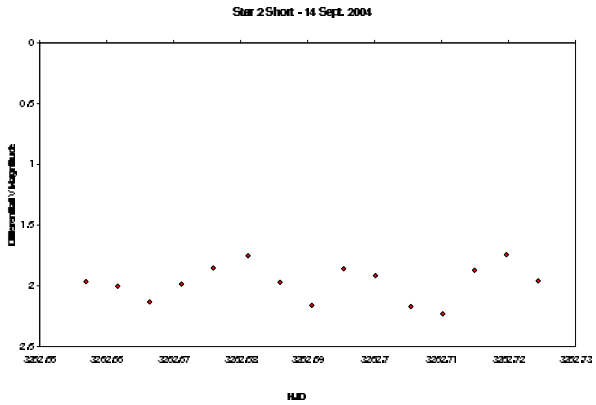

Figure 4.12 Light Curve for Star 2 Short, taken 14 Sept. 2004.

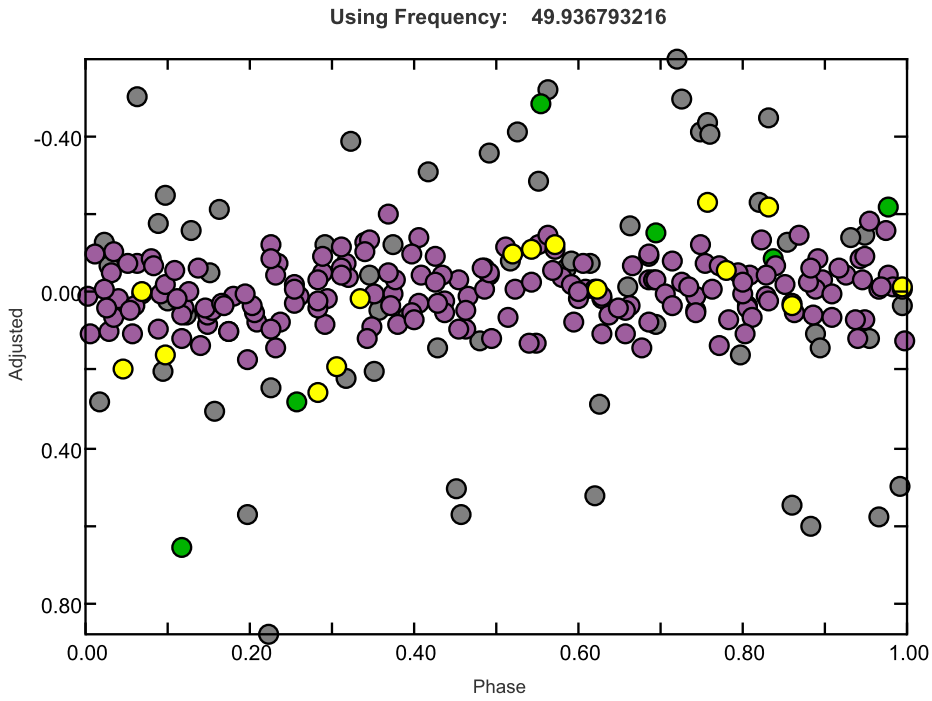

Figure 4.13 Phased Light Curves of Four Nights for Star 2 Short. Observed Phase Period: 0.036^d.

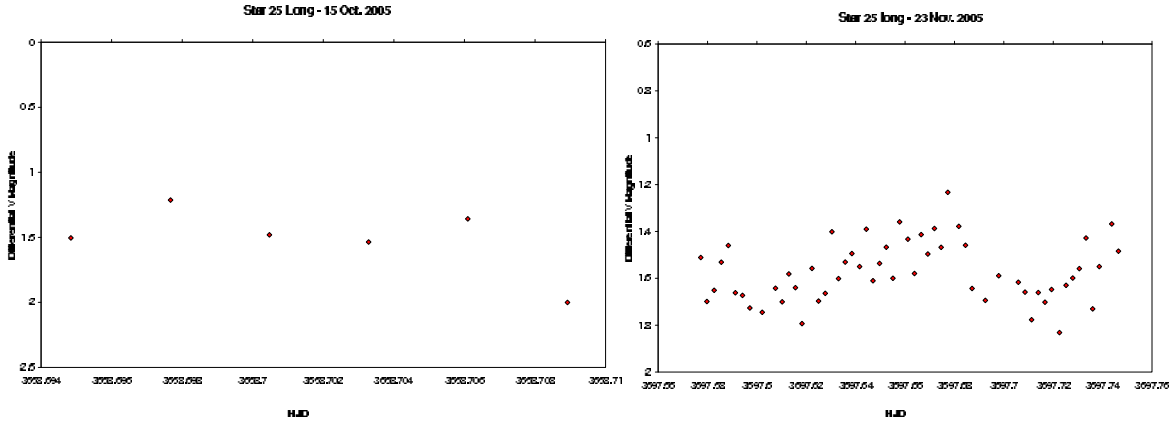

Figure 4.14 Light Curves for Star 25 Long, taken 15 Oct. 2005 and 23 Nov. 2005.

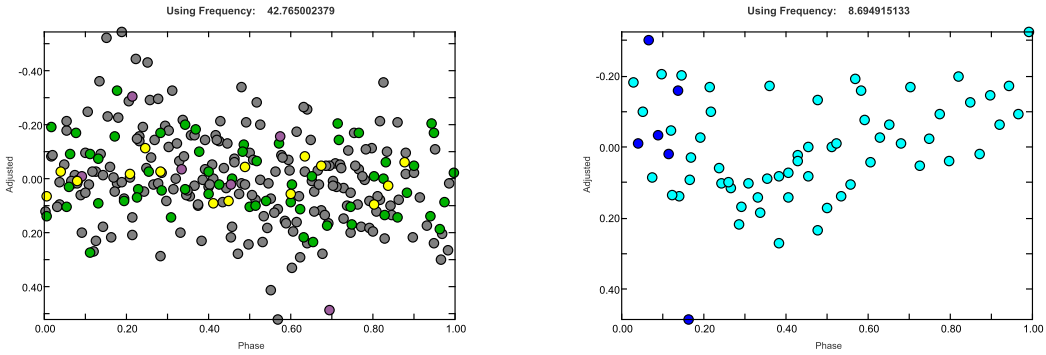

Figure 4.15 Phased Light Curves of Four and Two Nights, Respectively, for Star 25 Long. Observed Phase Periods: 0.02^d and 0.115^d.

4.2.4 Star 57 Long

As with Star 25 Long, 57 Long was phased twice, once with all four nights and once including only the cleanest two. In the first plot, a slight period can be made out among all the scatter while in the second a more obvious downward trend exists. Both phases resulted in very similar periods, however: those of 0.02794 and 0.028869 days (40 and 42 minutes, respectively). Due to the low predicted periods and noise-encumbered plots, 57 Long may not be as likely of a variable candidate as the others listed. However, its graph activity still warrants further future study. (See Fig. 4.16-18.)

4.2.5 Star 58 Long

Star 58 Long claims a potential period of 0.07805 days (1.87 hours). Its slight periodic phase plot is supported by its four nights of sinusoidal light curves. (See Fig. 4.19-21.)

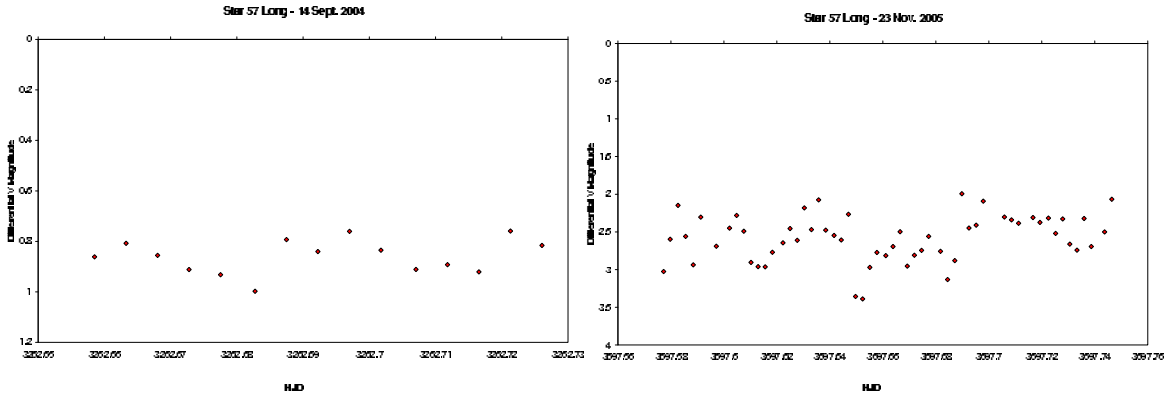

Figure 4.16 Light Curves for Star 57 Long, taken 14 Sept. 2004 and 23 Nov. 2005.

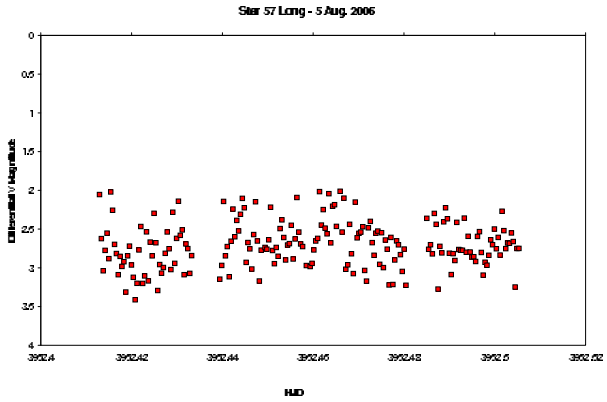

Figure 4.17 Light Curve for Star 57 Long, taken 5 Aug. 2006.

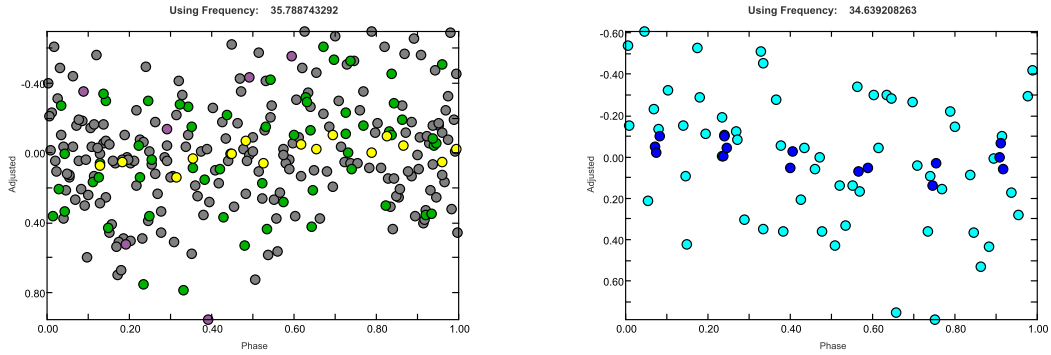

Figure 4.18 Phased Light Curves of Four and Two Nights, Respectively, for Star 57 Long. Observed Phase Periods: 0.0279^d and 0.028^d.

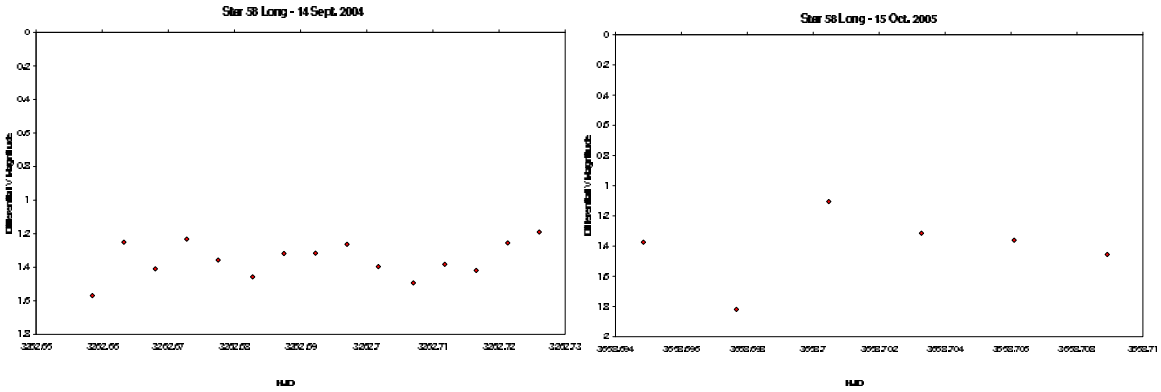

Figure 4.19 Light Curves for Star 58 Long, taken 14 Sept. 2004 and 15 Oct. 2005.

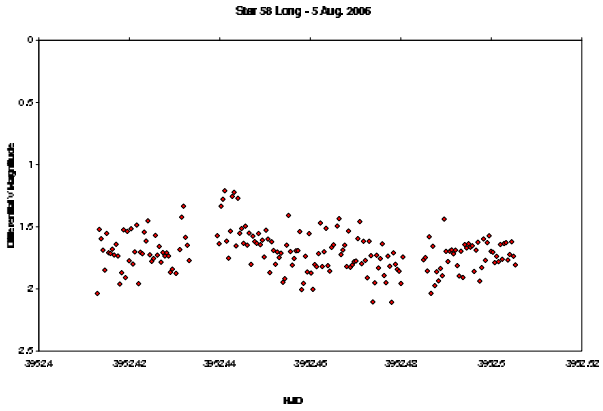

Figure 4.20 Light Curve for Star 58 Long, taken 5 Aug. 2006.

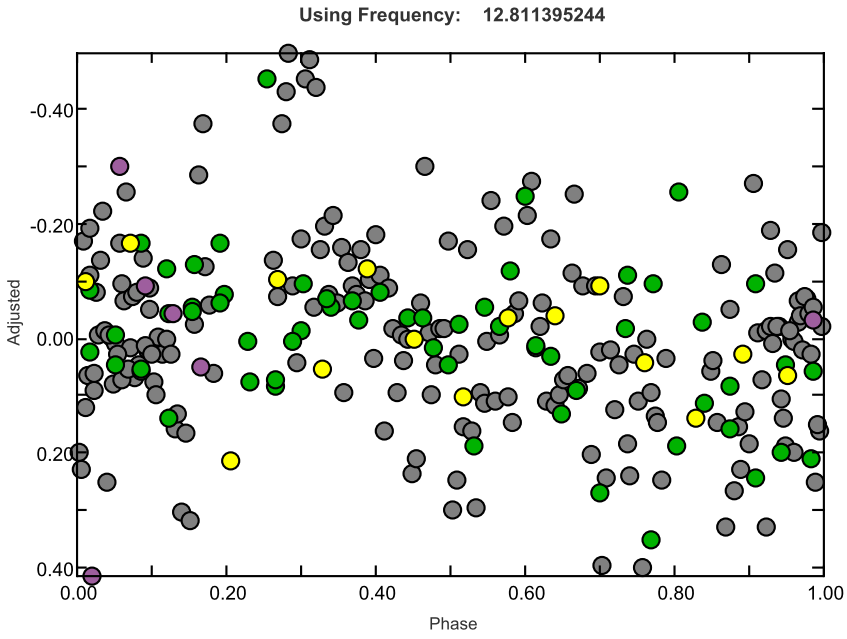

Figure 4.21 Phased Light Curves of Four Nights for Star 58 Long. Observed Phase Period: 0.078^d.

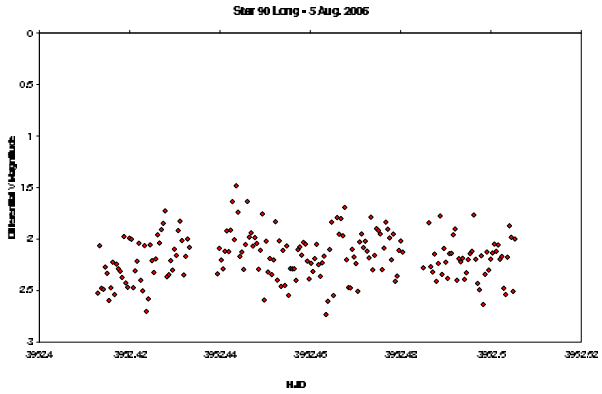

Figure 4.22 Light Curve for Star 90 Long, taken 5 Aug. 2006.

4.2.6 Star 90 Long

All four nights contributed well to Star 90 Long's phase plot, which yields a calculated period of 0.04066 days (almost 1 hour). (See Fig. 4.22-4.23.)

4.2.7 Star 96 Long / Star 25 Short

Though data for 96 Long appears viable with a period of 0.052925 days (1.27 hours) and yields plots characterized with smooth curves, it once again fails to match up to its short-exposure counterpart. Star 25 Short produces a period of 0.023 days, again most likely too low for a variable to be accurately observed with our equipment. Furthermore, its phase plot appears to be consistent in magnitude. More research will have to be conducted as to why our short and long pairs fail to match up. (See Fig. 4.24-26.)

4.2.8 Star 111 Long / Star 28 Short

Like our previous dual-field pairs, 111 Long and 28 Short don't match in period, with 0.049848 days (1.2 hours) for 111 Long and a significantly longer 0.141432 days (3.4 hours) for 28 Short. Unlike the last two sets, however, both stars appear distinctly

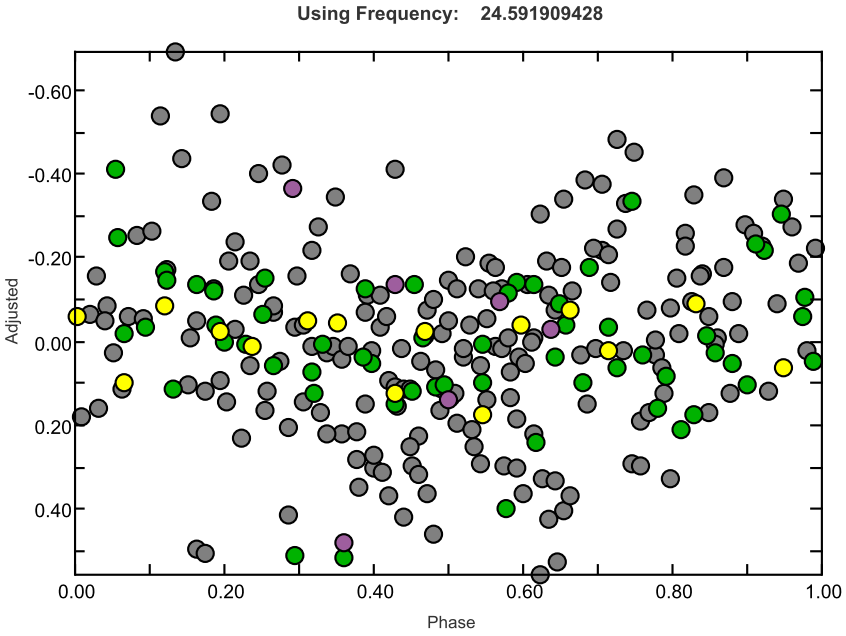

Figure 4.23 Phased Light Curves of Four Nights for Star 90 Long. Observed Phase Period: 0.04^d.

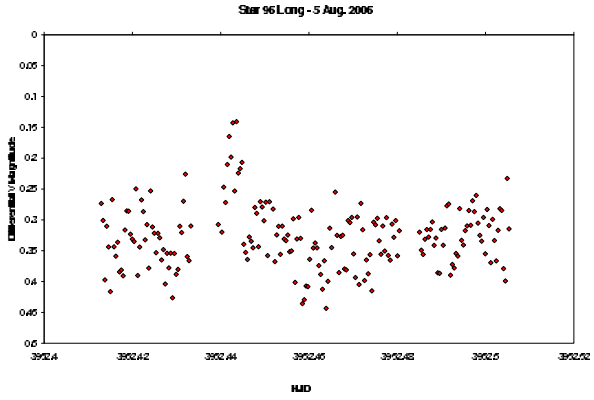

Figure 4.24 Light Curve for Star 96 Long, taken 5 Aug 2006.

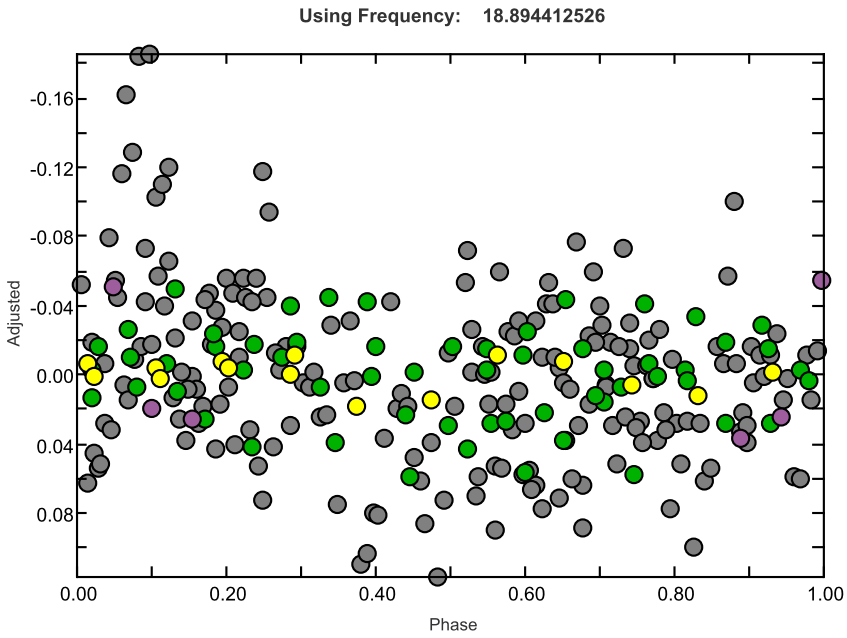

Figure 4.25 Phased Light Curves of Four Nights for Star 96 Long. Observed phase period: 0.05^d.

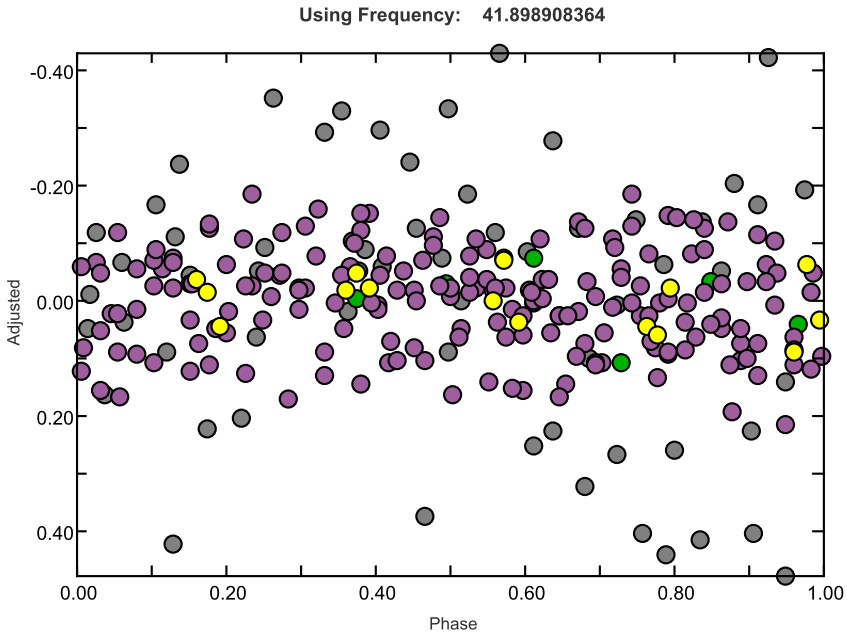

Figure 4.26 Phased Light Curves of Four Nights for Star 25 Short. Observed Phase Period: 0.023^d.

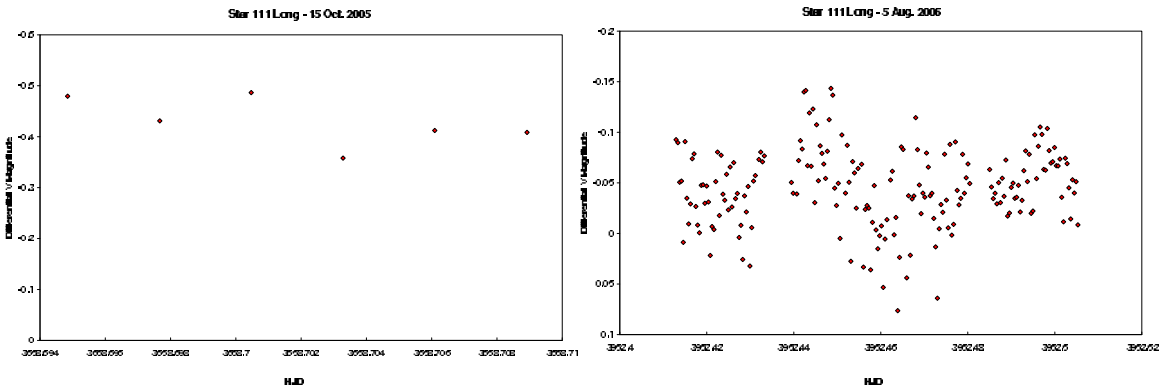

Figure 4.27 Light Curves for Star 111 Long, taken 15 Oct. 2005 and 5 Aug 2006.

variable. Light curves and phase diagrams are exhibited in figures Fig. 4.27-30.

4.2.9 Star 143 Long / Star 40 Short

All light curves and phase plots for Stars 143 Long and 40 Short proceed in a shallow, continuous undulation. The light curves' motion across the nights appears consistent with genuine variable motion, and would explain the relatively longer-than-mode periods of 0.154291 days (3.7 hours) for 143 Long and 0.137631 days (3.3 hours) for 40 Short. This periodic motion presents stable in all fields. When phased with all four nights, Star 143 long shows a shorter, though still smooth, period. The data from 14 Sept. 2004, not photometric in this particular area of the sky at that particular time of night, was removed to give us a second phase plot for 143 Long. The resultant period matches more closely to that obtained from the short field phase, and is therefore hypothesized as more legitimate. (See Fig. 4.31-34.)

4.2.10 Star 147 Long

Star 147 Long is interesting in that it fluctuates over a larger range of differential magnitude than any other studied here (Δm = 2). However, this characteristic only

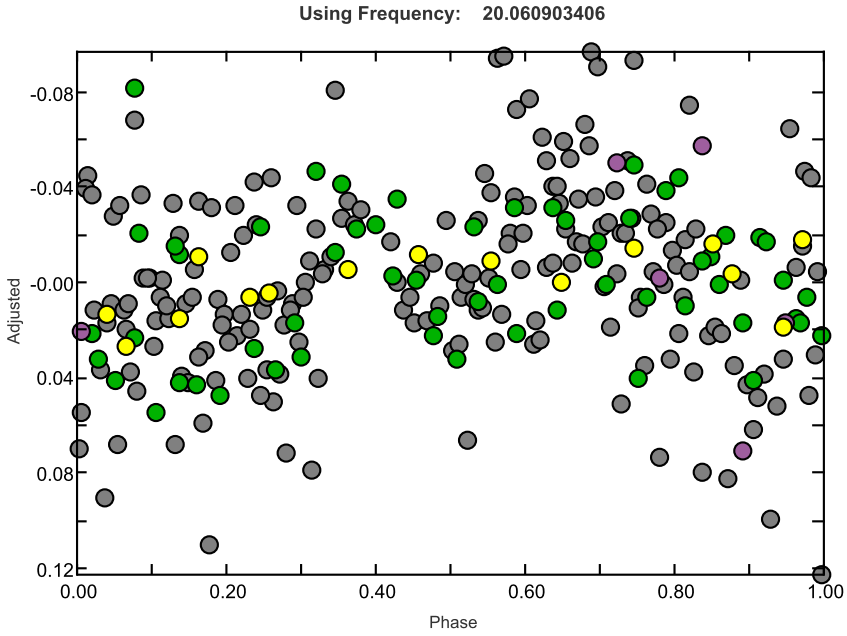

Figure 4.28 Phased Light Curves of Four Nights for Star 111 Long. Observed phase periods: 0.05^d.

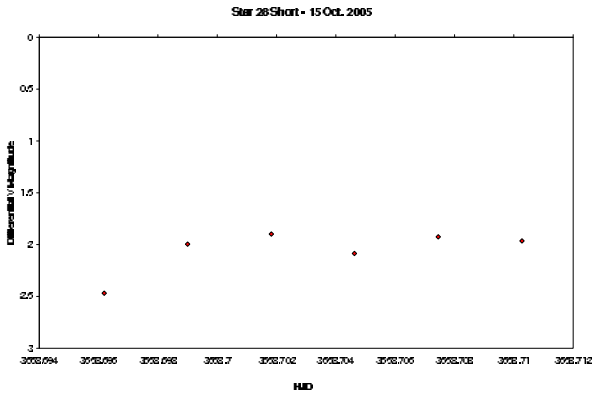

Figure 4.29 Light Curve for Star 28 Short, taken 15 Oct. 2005.

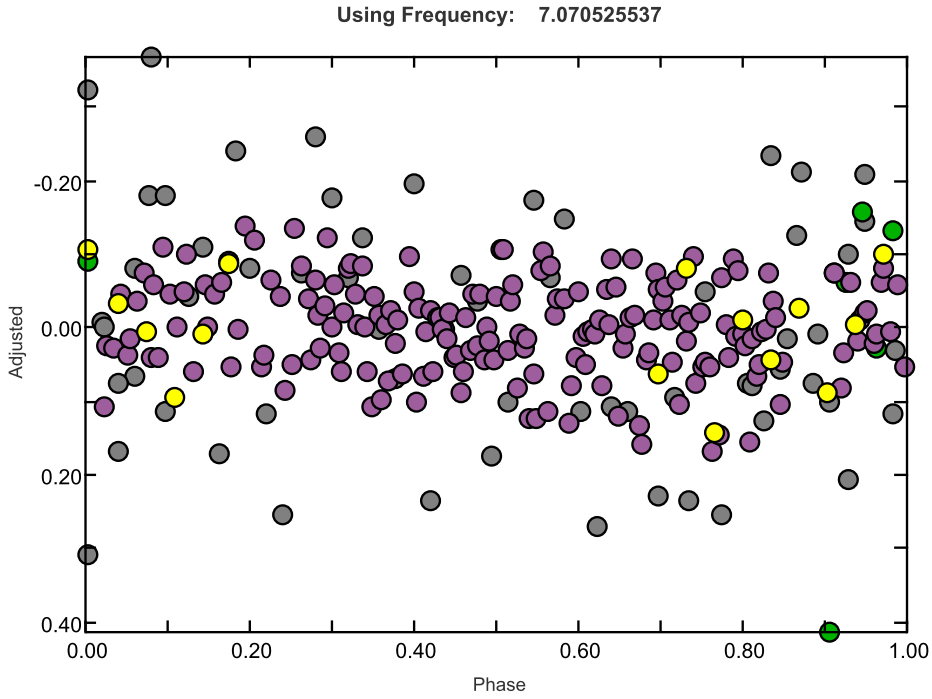

Figure 4.30 Phased Light Curves of Four Nights for Star 28 Short. Observed Phase Period: 0.14^d.

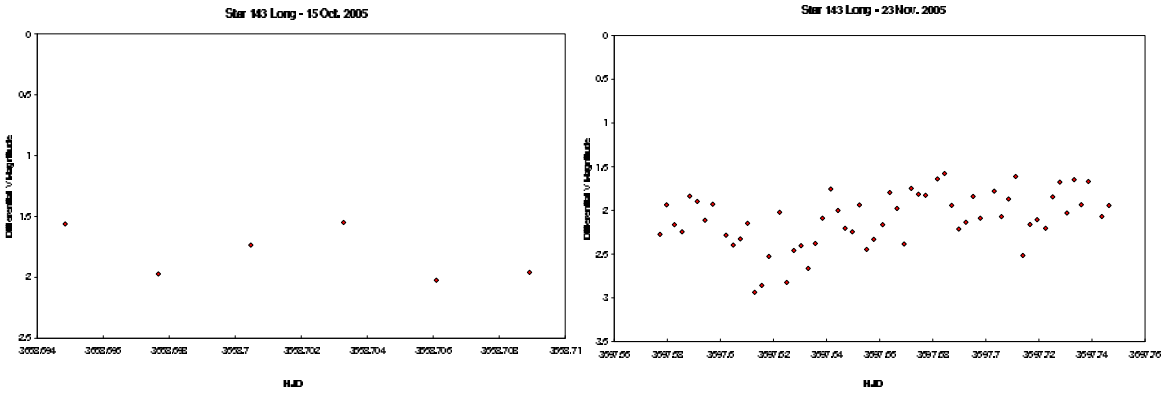

Figure 4.31 Light Curves for Star 143 Long, taken 15 Oct. 2005 and 23 Nov. 2005.

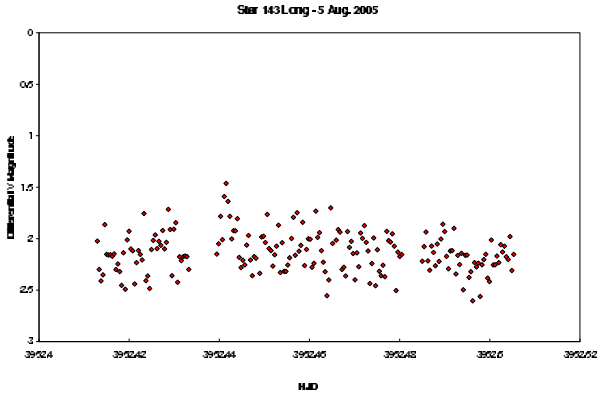

Figure 4.32 Light Curve for Star 143 Long, taken 5 Aug. 2006.

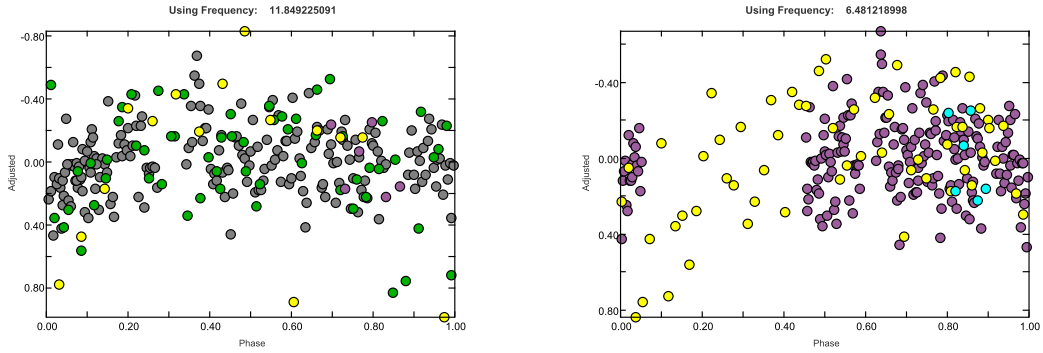

Figure 4.33 Phased Light Curves of Four and Three Nights, Respectively, for Star 143 Long. Observed Phase Periods: 0.08^d and 0.15^d.

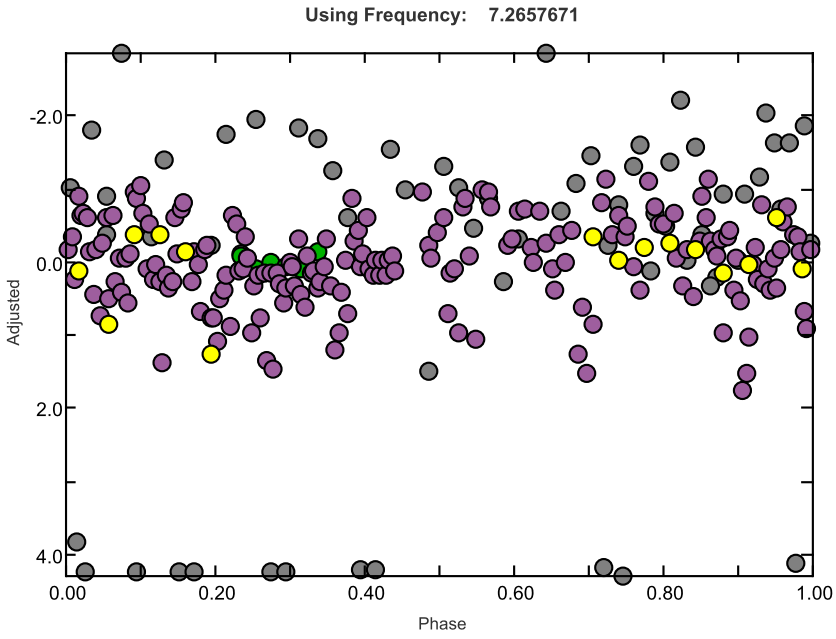

Figure 4.34 Phased Light Curves of Four Nights for Star 40 Short. Observed Phase Period: 0.13^d.

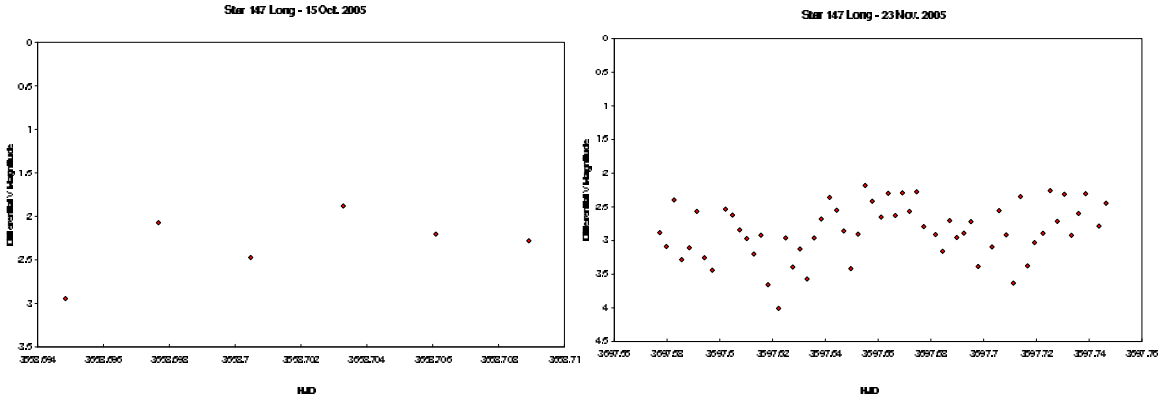

Figure 4.35 Light Curves for Star 147 Long, taken 15 Oct. 2005 and 23 Nov. 2005.

appears in two of our nights, those of 15 Oct. and 23 Nov. (see Fig. 4.35-36). A phase plot graphed with just the two nights yields a varying curve with a slightly different Δm and a period of 0.079308 days (almost 2 hours).

4.2.11 Star 163 Long

Based on Star 163 Long's continuously decreasing periodic movement, we hypothesize that it may be an eclipsing variable. Both phase plots, one containing all four nights and one stripped of the 14 Sept. data, yielded very similar periods of 0.078894 and 0.078831 days (1.89 hours). (See Fig 4.37-38.)

4.2.12 Star 164 Long

Star 164 Long presents with a calculated period of 0.088925 days (2.13 hours). All of its light curves demonstrate possible variability and its phase diagram covers a Δm of about 0.6. (See Fig. 4.39-41.)

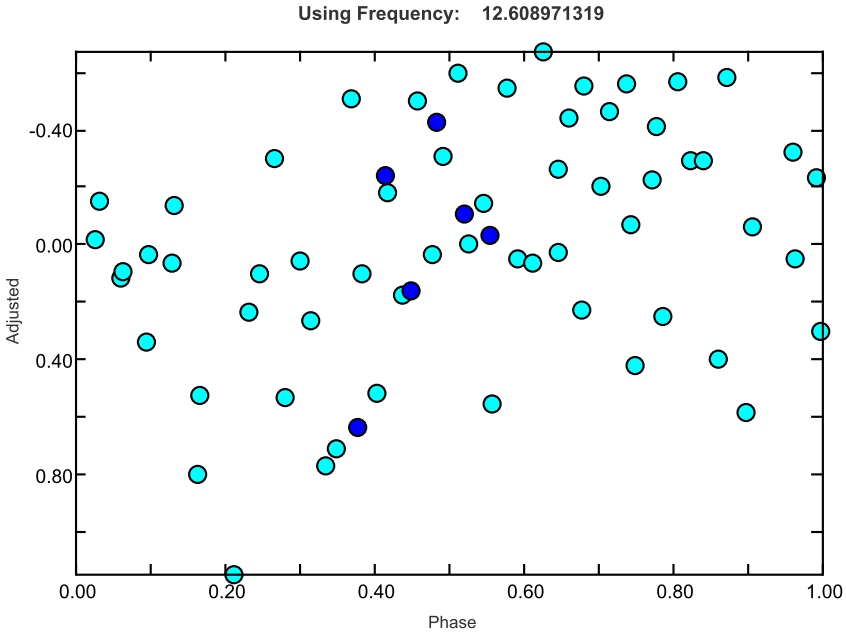

Figure 4.36 Phased Light Curve of Four Nights for Star 147 Long. Observed Phase Period: 0.079^d.

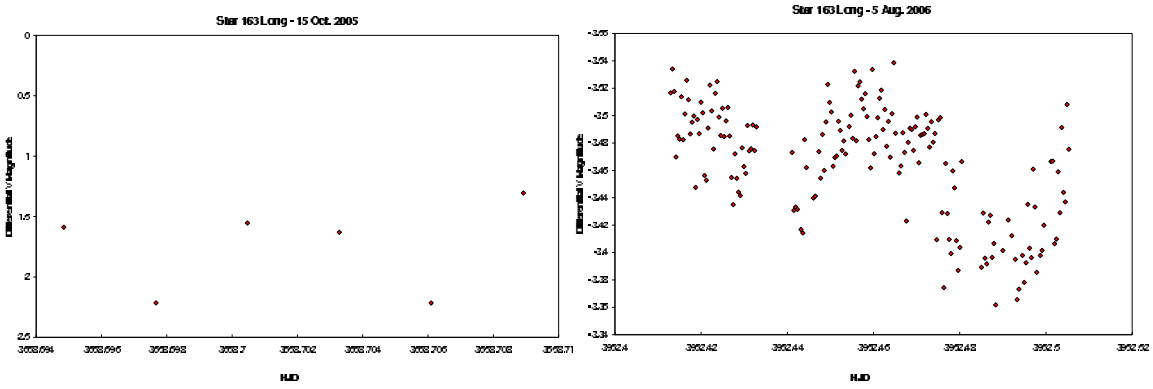

Figure 4.37 Light Curves for Star 163 Long, taken and 15 Oct. 2005 and 5 Aug. 2006.

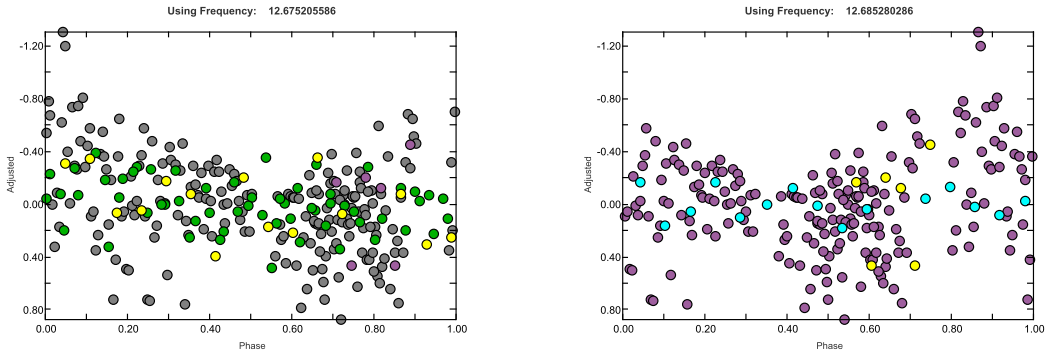

Figure 4.38 Phased Light Curves of Four and Three Nights, Respectively, for Star 163 Long. Observed Phase Periods: both 0.078^d.

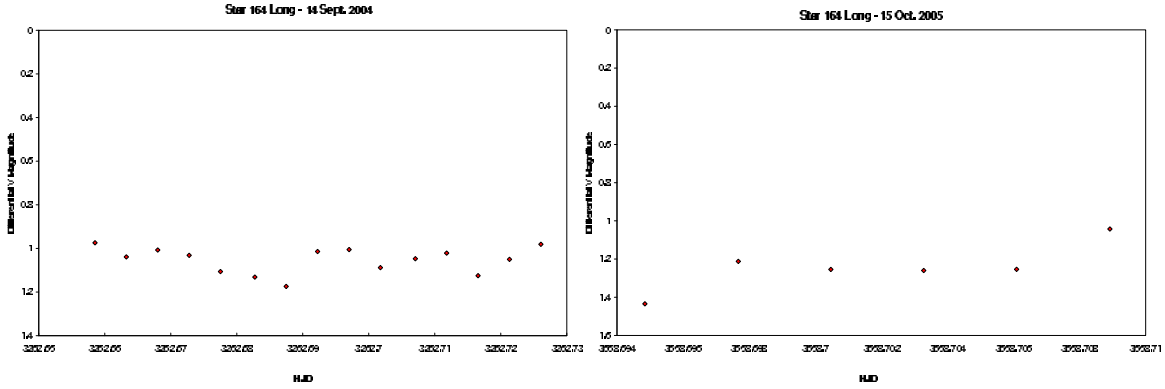

Figure 4.39 Light Curves for Star 164 Long, taken 14 Sept. 2004 and 15 Oct. 2005.

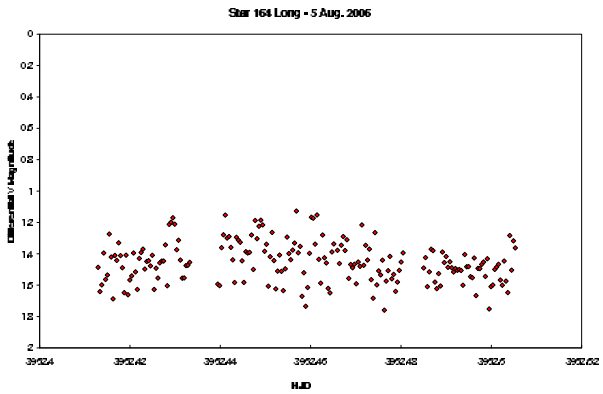

Figure 4.40 Light Curve for Star 164 Long, taken 5 Aug. 2006.

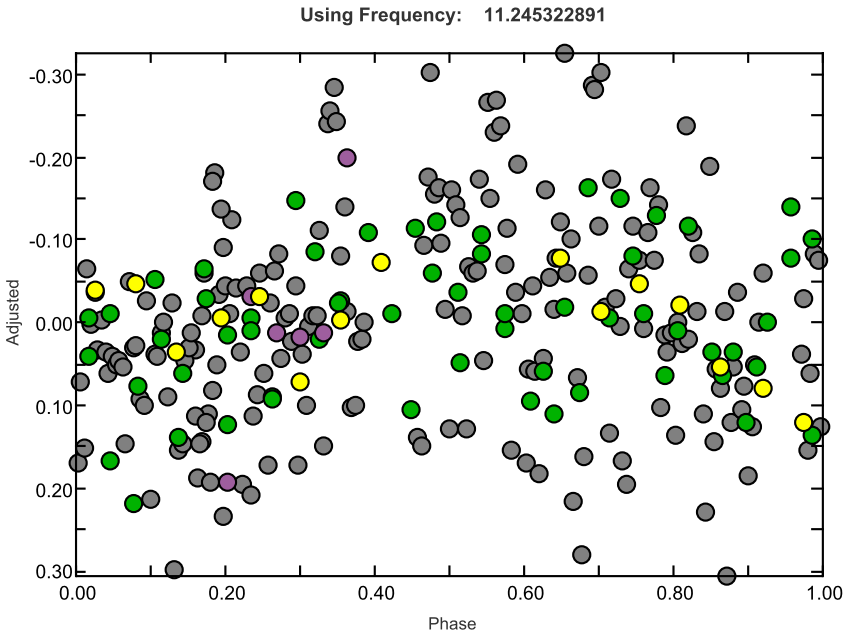

Figure 4.41 Phased Light Curves of Four Nights for Star 164 Long. Observed Phase Period: 0.088^d.

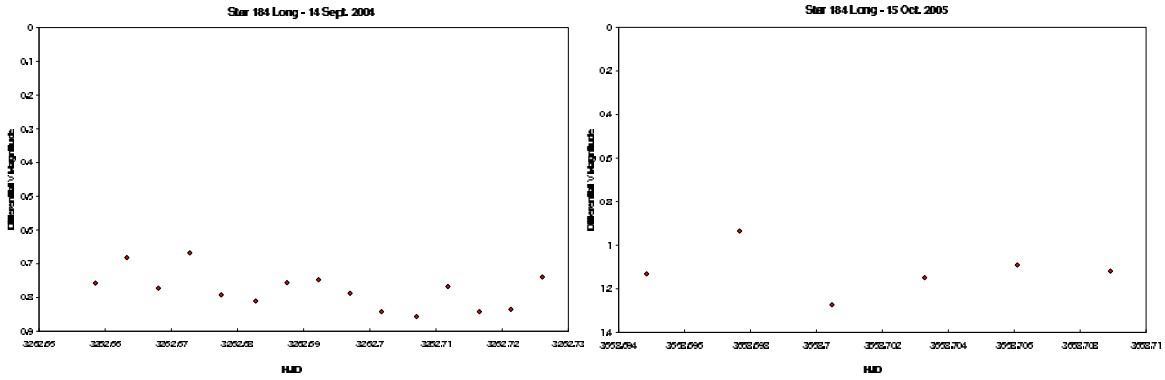

Figure 4.42 Light Curves for Star 184 Long, taken 14 Sept. 2004 and 15 Oct. 2005.

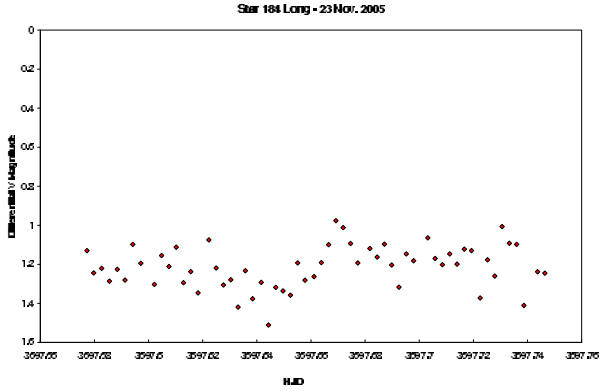

Figure 4.43 Light Curve for Star 184 Long, taken 5 Aug. 2006.

4.2.13 Star 184 Long

Due to minor inconsistencies in the field of view of data taken at the Orson Pratt Observatory as opposed to that of the West Mount Observatory, no data was collected at West Mount (6 Aug) for this star. As a result, our phase diagram includes only three nights, but still appears to demonstrate variation with a solid period of 0.129246 days (3.1 hours). (See Fig. 4.42-44.)

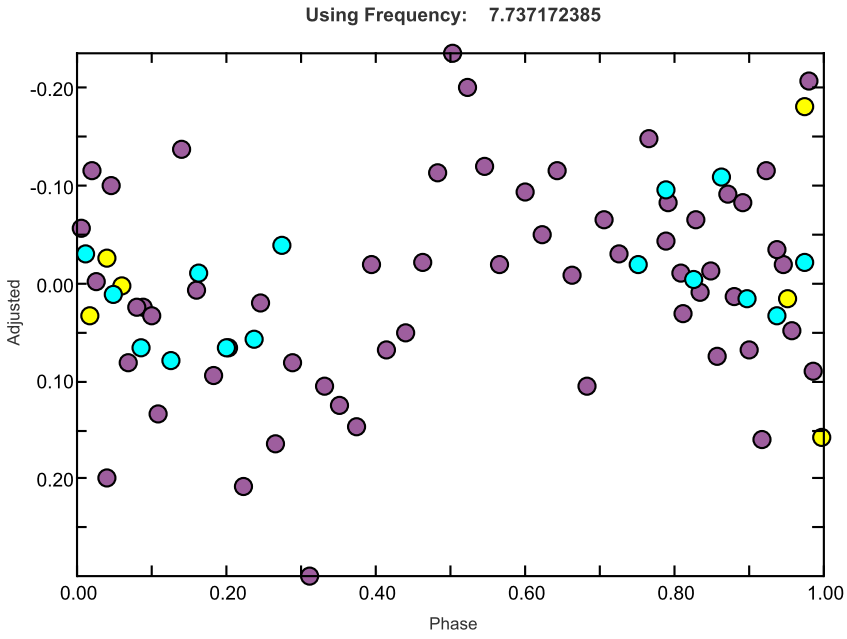

Figure 4.44 Phased Light Curves of Three Nights for Star 184 Long. Observed Phase Period: 0.129^d.

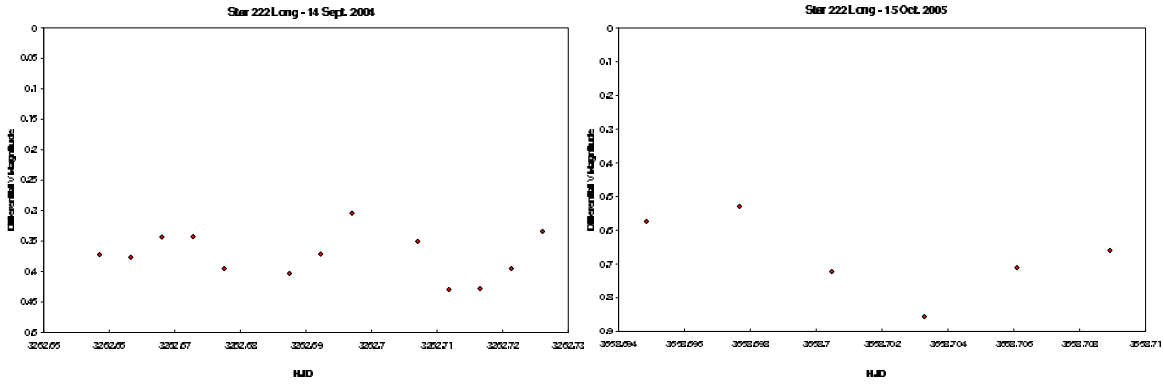

Figure 4.45 Light Curves for Star 222 Long, taken 14 Sept. 2004 and 15 Oct. 2005.

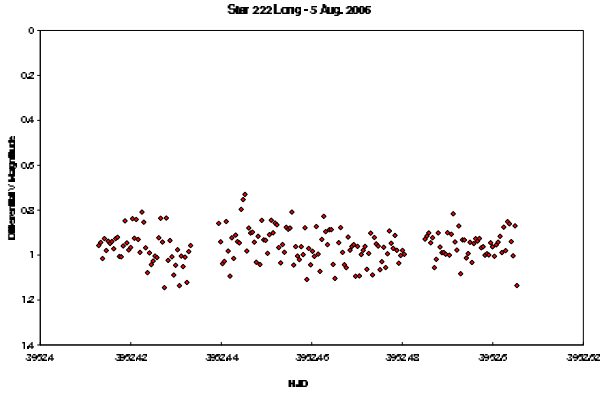

Figure 4.46 Light Curve for Star 222 Long, taken 5 Aug. 2006.

4.2.14 Star 222 Long

Star 222 was phased in four and three nights of data; both returned similar periods of 0.037627 and 0.039643 days (54 and 57 minutes). The second phase plot, minus the 23 Nov. data, slopes a bit more steeply than that of all four nights, but holds the same general form. Because both phases gave such similar periods, we assume that the only difference attributed by the addition of the 23 Nov. data is that of slightly less photometric conditions. Otherwise, it seems as if the star behaved consistently throughout all four nights. (See Fig. 4.45-47.)

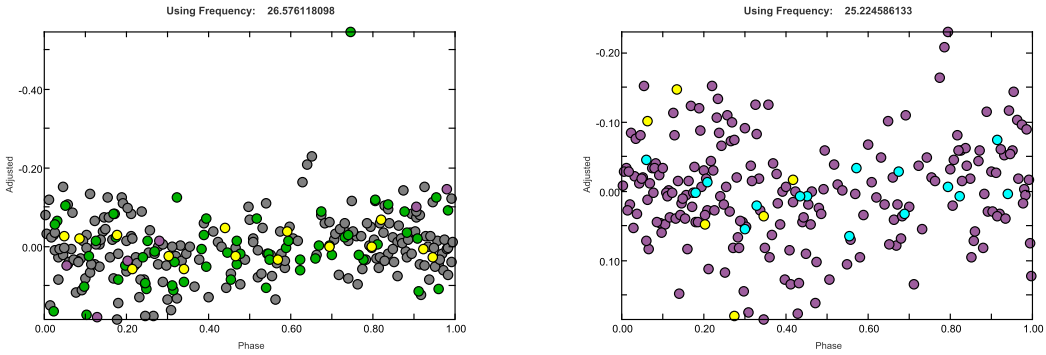

Figure 4.47 Phased Light Curves of Four and Three Nights, Respectively, for Star 222 Long. Observed Phase Periods: both 0.03^d.

4.2.15 Star 42 Short

Star 42 Short's best light curves, unfortunately, are made up of those nights with the fewest data points taken. Therefore, even though their curves appear to follow a legitimately variable path, their variability cannot be sufficiently proven without further research. Furthermore, a phase diagram of all four nights yields inconclusive data: a plot with a small hiccup near the beginning, but apparently flat for the remainder. A second plot of its two best nights presents a better-looking curve, but again, there are too few points to draw any sound conclusions. Both plots, however, yielded periods consistent with the trend: 0.0416299 days (1 hour) and 0.0352147 days (50 minutes). (See Fig 4.48-49.)

4.3 Conclusions and Future Research

The section of M39 that we studied proved to be relatively rich in variables. Aside from verifying fluctuating action in the three known variables, Stars 72, 77, and 81 Short, we discovered 10 probable variables and 5 possible. Of the probable, Stars 10 and 24 Long exhibit excellent phase plots and periods, though 24 Long's short-

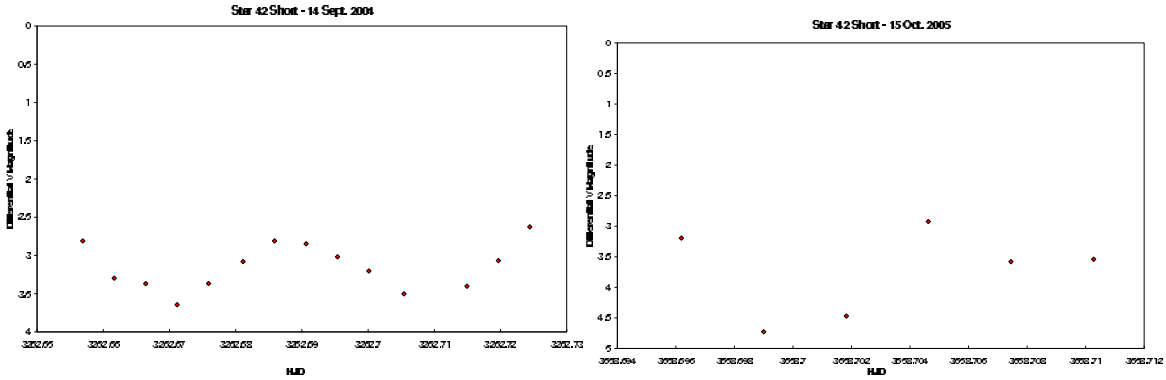

Figure 4.48 Light Curves for Star 42 Short, taken 14 Sept. 2004 and 15 Oct. 2005.

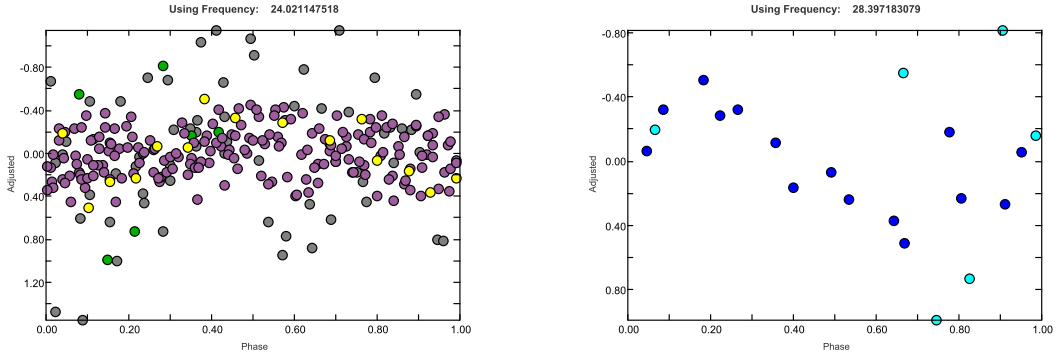

Figure 4.49 Phased Light Curves of Four and Two Nights, Respectively, for Star 42 Short. Observed Phase Periods: 0.04^d and 0.035^d.

exposure counterpart, 2 Short, appears flat when phased for reasons likely attributable to errors inherent in the observation or reduction process. Stars 58 and 90 Long also show obvious periodic motion. The 111 Long / 28 Short and 143 Long / 40 Short pairs hold up well when graphed, though 111 Long/28 Short differ in period by quite a large margin. Stars 163, 164, 184, and 222 also demonstrate strong variable tendencies.

Of the possible, 25 Long exhibits slight tendencies toward variation, whereas 2 Short presents definite fixed luminosity. It would be interesting to discover why one data set of what is supposedly the same star strays so drastically from the behavior of its partner. A shallow period can be seen in Star 57 Long. Star 96 Long / 25 Short and 147 Long show well-defined light curves, but fail to make a convincing phase. Star 42 Short's phase presents a decent shape but is made of too few points to be truly conclusive.

Room for future projects lies in every one of these variable candidates. Of the possible variable group, a higher frequency and length of nights can be observed and reduced in the same manner as this thesis in order to definitively categorize them into one family or another. Of the probable variable group, work that was beyond the scope of this thesis—such as spectroscopic or more precise and powerful photometric observations—can be performed. Our data were taken in three separate filters, but were not analyzed for this particular project; filter data could add a lot to understanding other aspects of our variables' stellar properties. It would also be interesting to determine classification for each variable and compile them into a larger data set, useful for searching out trends and patterns in the whole of M39. A determination such as this, applied to clusters and celestial objects on a grander scale, would lead us not only further down the path of understanding stellar evolution, but scientific progression as well.

Bibliography

[1] B. D. Broadbent, Senior's thesis, Brigham Young University, 2006.

[2] T. C. Bush, Senior's thesis, Brigham Young University, 2005.

[3] K. E. Moncrieff, Senior's thesis, Brigham Young University, 2005.

[4] G. S. Zeilik, M., Introductory Astronomy and Astrophysics **4,** 352–368 (1997).

[5] "$http://www.univie.ac.at/tops/Period04/$,".

[6] "GCVS, $http://www.sai.msu.su/groups/cluster/gcvs/$,".

[7] F. Rufener, AsAp No. 3 (1971).

[8] "AAVSO, $http://www.aavso.org/$,".

[9] A. G. I. R. Y. Zakirov, M.M., IBVS **4220,** 1 (1995).

[10] F. Rufener, AsAp **2,** 242–252 (1981).